Astron. Astrophys. 224, 225–241 (1989)

ASTRONOMY AND ASTROPHYSICS

The origin and the diagnostic capabilities of the Stokes V asymmetry observed in solar faculae and the network

S.K. Solanki

Department of Mathematical Sciences, University of St. Andrews, St. Andrews, KY16 9SS, Scotland

Received February 27, accepted March 30, 1989

Summary. Strokes profiles of four spectral lines with widely different properties are calculated in a two dimensional flux tube model of a solar magnetic element. The model satisfies pressure balance and has empirically derived temperature and magnetic field strength values within the magnetic element. Various model parameters (e.g. internal and external temperatures, velocity amplitudes and gradients, flux tube geometry etc.) are varied and their influence on the Stokes V asymmetry and other line parameters is studied. The asymmetry is the Stokes V line parameter most strongly affected by the non-magnetic part of the atmosphere. Other Stokes V parameters are much less affected by the details of the external atmosphere, e.g. the absolute areas or amplitudes of the Stokes V wings respond only mildly to changes in the external temperature. Furthermore, the Stokes V width is almost independent of external stationary and non-stationary velocities, so that velocity amplitudes previously derived from the Stokes V line width (e.g. Solanki, 1986) must refer to mass-motions within the magnetic elements. This makes the Stokes V asymmetry an important diagnostic of the close surroundings of magnetic elements. It is also a valuable diagnostic of mass-motions inside magnetic elements.

The considered model can reproduce the blue-red Stokes V asymmetry along with other line parameters observed near disk centre in solar active region plages and the network if it incorporates the following three features: 1) A downflow of $0.5-1.5\ \mathrm{km\,s^{-1}}$ in the immediate surroundings of the flux tube (but not inside it). 2) A 250–350 K lower temperature in the downflowing non-magnetic atmosphere than in the average quiet sun. 3) A longitudinal wave-like or oscillatory motion with an amplitude of between 1 and $3\ \mathrm{km\,s^{-1}}$ within the magnetic element. Thus the Stokes V asymmetry is seen to be a natural outcome of the current picture of magnetic elements embedded in cool downflowing intergranular lanes. The model calculations also provide strong observational evidence for the presence of relatively large amplitude non-stationary mass motions within magnetic elements and may suggest that the temperature in the upflowing and the downflowing phases is not the same, possibly due to radiative damping.

These results are discussed in the context of investigations published in the literature. Their implications for 1-D models of magnetic elements and the Stokes profiles calculated therewith the elucidated. It is shown that although for some aims the Stokes V profiles resulting from 1-D models are sufficiently accurate, the 1-D approximation is totally inadequate for the quantitative analysis of Stokes V asymmetry.

Key words: The Sun: magnetic fields – photosphere – faculae – Stokes profiles

1. Introduction

The stokes V profiles observed in active region plages and in the quiet solar network exhibit a pronounced asymmetry (e.g. Stenflo et al., 1984; Wiehr, 1985). Near solar disk centre almost all spectral lines have Stokes V profiles whose blue wings are stronger than their red wings (e.g. Solanki and Stenflo, 1984, 1985), i.e. $\delta A>0$ and $\delta a>0$. δA is the relative area asymmetry defined as $\delta A=(A_b-A_r)/(A_b+A_r)$ with A_b and A_r being the unsigned areas of the blue and red wings of Stokes V. δa is the relative amplitude asymmetry defined as $\delta a=(a_b-a_r)/(a_b+a_r)$, where a_b and a_r are the unsigned blue and red Stokes V amplitudes.

Until recently the source of this asymmetry has been rather enigmatic. Although various mechanisms have been proposed to explain these observations, none has so far reproduced the data consistently within the framework of a physically reasonable model. The mechanisms can be grouped into two basic categories: those involving velocity gradients (e.g. Illing et al., 1975; Auer and Heasley, 1978) and those based on atomic orientation in cases of thermodynamic non-equilibrium (i.e. NLTE, Kemp et al., 1984; Landi Degl'Innocenti, 1985). Due to its great complexity, the atomic orientation model has never been applied quantitatively to the solar case.

The velocity gradient scheme exists in numerous variants. The simplest of these is based on a steady flow inside a 1-D model of the magnetic elements. One of the naturally expected properties of V profiles calculated using such models is that their zero-crossing wavelengths should be shifted by the steady flow, in contrast to recent observations which find no such shifts (e.g. Stenflo and Harvey, 1985; Solanki, 1986; Solanki and Pahlke, 1988). However, it has been shown that for a magnetic field strength B increasing with height and a downflow velocity v decreasing with height asymmetric Stokes V profiles with small zero-crossing shifts can be produced (Sánchez Almeida et al., 1988). Unfortunately, such a field strength variation conflicts with both MHD force balance (e.g. Deinzer et al., 1984a, b; Steiner et al., 1986; Knölker et al., 1987; Steiner and Pizzo, 1989) and observational data (Stenflo et al., 1987b; Zayer et al., 1989). For physically reasonable magnetic field (i.e. a field strength decreasing with height) and velocity structures this scheme has been

demonstrated by Solanki and Pahlke (1988) to produce profiles which conflict with the observed zero-crossing wavelengths. In another paper Sánchez Almeida et al. (1989) show that it is, in principle, possible to reproduce the absolute area asymmetry $(A_b - A_r)$ of multiple spectral lines with such a model, if the rest of the line parameters are ignored. In contrast, Solanki and Pahlke (1988) have found that such models, with empirically derived temperature structures, cannot simultaneously reproduce the asymmetries of spectral lines having widely different excitation energies or strengths in the magnetic element (i.e. different amounts of saturation). In summary, the situation with models based on the gradients of stationary flows within magnetic elements is unclear. They appear to be workable if a free choice of model parameters is allowed, but when a little more realism is introduced by restraining atmospheric parameters to physically and observationally acceptable values, they do not work. It appears extremely difficult to reconcile all the observed Stokes V parameters with the results of these models, and I shall not consider them further in the present paper. The work of Sánchez Almeida et al. (1989) is valuable, however, in that it suggests, that in one form or another velocity gradients do lie at the heart of the Stokes V asymmetry.

Another variant of the velocity gradient scheme is due to Van Ballegooijen (1985b), who pointed out that downflows outside magnetic elements can also produce a Stokes V asymmetry having the correct sign of δA if the expansion of the magnetic elements with height is taken into account. An expansion with height is a feature of all models of magnetic elements incorporating MHD force balance and flux conservation. Grossmann-Doerth et al. (1988, 1989b) have shown that in this model, when B and v are nowhere cospatial, Stokes V profiles can be asymmetric *without exhibiting any zero-crossing wavelength shift at all*, thus overcoming one of the key observational hurdles without compromising physical consistency. However, no attempt was made by the above authors to quantitatively reproduce, e.g., the asymmetry of more than one Stokes V profile, or the correct ration of δa to δA. In the present paper I, therefore, attempt a first simple quantitative fit to the data with this promising model.

Non-stationary mass-motions within the magnetic elements have also been proposed as a source of the Stokes V asymmetry (e.g. Solanki and Stenflo, 1984), but their influence has never been studied quantitatively. Since, additionaly, there are strong theoretical ground for expecting such motions, I also explore how they create Stokes V asymmetry with the help of a simple two time-components model of wave-like or oscillatory motions. Particular emphasis is placed on studying the combined effect of oscillations within the magnetic elements and downflows external to them. Such combined models are able to remove the main remaining discrepancies between the observations and the model with downflows outside the magnetic elements only.

Any successful attempt to reproduce the observed asymmetry with the help of model calculations also provides additional information on the magnetic elements and their surroundings, i.e. the Stokes V asymmetry serves as a diagnostic of solar magnetic elements. The exploration of these diagnostic capabilities at solar disk centre, which promise to provide exciting new insight into the physical structure of the atmosphere inside and in the immediate surroundings of solar magnetic elements, is the other major topic of the present paper.

Since most of the calculations are carried out within the general context of simple flow fields within and outwith the magnetic elements, they must be considered exploratory in nature and the results somewhat preliminary. In general, I shall discuss only the Stokes V profile. The potentially equally interesting Stokes I asymmetry (line bisectors) is not discussed further, since the present model does not incorporate an upflowing region outside the magnetic elements (granule centres), without which no reasonable Stokes I line shapes can be produced.

2. Model, method and data

2.1. Simple hydromagnetic model

The model is composed of a magnetic flux tube which expands with height. It is surrounded by and partly overlies a downflowing non-magnetic atmosphere.

The magnetic field strength, B, within the flux tube is calculated by imposing exact horizontal pressure balance, i.e. using the thin tube approximation (e.g. Defouw, 1976; Roberts and Webb, 1979; Parker, 1979), with a horizontally constant field strength and gas pressure within the flux tube and a sharp boundary to the non-magnetic atmosphere (cf. Schüssler, 1986; Knölker et al., 1988, and Zayer et al., 1989, for arguments and evidence in favour of relatively sharp boundaries with thin current sheets). For small magnetic elements and realistic temperatures, a model based on the thin tube approximation differs only slightly from models including magnetic tension (Pneuman et al., 1986; Knölker et al., 1988; Steiner and Pizzo, 1989). It is also complies well with the most sensitive observational field strength indicators in the lower and middle photosphere (Zayer et al., 1989). $B = 2000$ G has been chosen at $\tau = 1$ within the flux tube, in accordance with various observational diagnostics (Solanki et al., 1987, 1989; Zayer et al., 1989). Since the field strength decreases approximately exponentially with height, the area F of the flux tube must increase approximately exponentially with height, since flux conservation in the thin tube approximation demands BF to be constant. Except for a few test calculations, for which a slab geometry is assumed, a cylindrically symmetric model is used. In this model the radial component of the field, B_r, is calculated from the vertical component using

$$B_r = -\frac{r}{2}\frac{\partial B_z}{\partial z}$$

All calculations in the present paper refer to solar disk centre, so that the diameter of the vertical thin flux tube model need not be explicitely specified.

The atmosphere outside the magnetic element is initially represented by a model of the quiet sun, the HSRASP (Gingerich et al., 1971; Spruit, 1974; Chapman, 1979), modified such that the temperature in the chromospheric layers is parallel to the Holweger and Müller (1974) model (LTE approximation). Later, other temperature profiles are also used. These are constructed by increasing or decreasing $T(\tau)$ of the modified HSRASP, without changing the temperature gradient. τ signifies the continuum optical depth at 5000 Å. Thus a series of models is created which possess $T(\tau)$ profiles parallel to those of the modified HSRASP. These models are not self-consistent, since the other physical parameters of the HSRASP are left unchanged. For the simple exploratory calculations presented here such an approximation appears reasonable. The temperature structure inside the flux tube is generally taken to be the empirically derived network flux tube model of Solanki (1986). Other temperature structures have

also been used. Examples are, the plage flux tube model of Solanki (1986), or models with $T(\tau)$ parallel to the temperature stratification of the HSRASP, which are constructed similarly to the models of the non-magnetic atmosphere described above. $B(\tau=1)=2000$ G in all the flux tube models.

The flow outside the flux tube is assumed to be purely vertical and is directed downwards in almost all the calculated examples. A purely vertical velocity is not unduly restrictive, since at solar disk centre the line profiles are not affected by horizontal flows. The usual sign convention is used and downflows are represented by positive velocities. Three different depth profiles are tried for the flow velocity. It can either be independent of height, change linearly with height throughout the non-magnetic atmosphere, or change linearly within a "boundary layer" of a given vertical thickness near the walls of the flux tube and remain constant farther away. For most calculations a constant microturbulence of 0.8 km s^{-1} both outside and inside the flux tube is assumed, but some calculations have also been carried out with other microturbulence values.

A provision is made for allowing flows inside the flux tube. The influence of internal waves and oscillations is modelled in a very simple manner by assuming a two time-component model, one each for the upflow and the downflow phases. The velocity is kept constant for the duration of each phase and is also assumed to be independent of height in the atmosphere. Both phases have equal but opposite velocities. None of the other atmospheric parameters is changed. Once more, such a treatment is physically not completely self-consistent, but it allows a simple and efficient determination of basic influences on the Stokes V profile shape. Models with two or three velocity-components have been used extensively in the past to model the solar granulation (e.g. Keil, 1980; Immerschitt and Schröter, 1989). The influence on Stokes profiles of flux tube waves modelled in a more physically realistic manner is the subject of a separate investigation.

2.2. *Radiative transfer*

Once the hydromagnetic part of the model is determined it is intersected at various distances from the symmetry axis (or for slab geometry, the central plane) by a number of vertical rays or lines of sight. Along each of these the continuum optical depth is determined and the Stokes profiles are calculated numerically in LTE, using a greatly modified and extended version of the code described by Beckers (1969a, b; more details are given by Solanki, 1987c). The code includes a scheme by which the τ intervals are decreased in those parts of the atmosphere where the Stokes absorption coefficients become large or when changes in the transfer equation coefficients, induced by changes in the atmosphere, become significant. Such a procedure gives stable Stokes profiles in the overwhelming majority of the cases at considerably smaller computational cost than using standard techniques (e.g. repeating runs with two different τ intervals). Some form of numerical stabilisation is necessary, due to the strong gradients in the atmospheric parameters at the flux tube boundary. Next, each constituent profile is weighted according to the area represented by the ray along which it is formed. Then, the average is calculated of all the profiles formed within a given radius from the centre of the flux tube. For symmetry reasons, it is sufficient to consider only the rays passing through half a plane at solar disk centre. Finally, the average Stokes V profile is divided by the average continuum intensity, before being compared with the observations. A 2-D model and the averaging over many rays is essential due to the limited spatial and temporal resolution of the observational data. Generally 12–15 rays have been chosen. For test purposes, some calculations with more rays have also been carried out. The results are sufficiently similar to warrant taking the more economical number, although the calculations with the smaller number of rays tend to produce larger asymmetries.

In the present model only the Stokes V profiles formed along rays which pass through the flux tube boundary have an area asymmetry $\delta A \neq 0$. In the following I shall call this outer part of the flux tube the "canopy", while the inner part, where the Stokes V profiles have $\delta A=0$, is named the "central cylinder". 1-D models generally represent only the central cylinder. Note that when moving downwards along one of the canopy rays there is a sharp drop in B and a sharp rise in v when it passes through the canopy boundary. The "canopy" defined here should not be confused with the larger and generally higher structures so named by Giovanelli (1980) and reviewed by Jones (1985).

2.3. *Selected spectral lines*

For the present analysis I have selected four of the spectral lines used in an earlier study of Stokes V asymmetry by Solanki and Pahlke (1988). The lines and some of their atomic parameters are listed in Table 1. χ_e is the excitation potential of the lower level of the transition, $g_{\rm eff}$ is the effective landé factor in LS coupling, and $\log g^* f$ is the logarithmic, statistically weighted oscillator strength. The Landé factors obtained from laboratory measurements are very close to the LS coupling values for all four lines (Solanki and Stenflo, 1985). $\log g^* f$ values are taken from laboratory measurements by Blackwell et al. (1979a, b) for the three Fe I lines and from a compilation of values by Phillips (1979) for the Fe II line. The damping constants, calculated using the Unsöld (1955) formula, are enhanced by factors ranging from 1 to 2.5 in accordance with Holweger (1979) and Simmons and Blackwell (1982). The three Fe I lines have similar (low) excitation potentials, but widely different equivalent widths in the quiet sun, so that they are greatly weakened by higher temperatures and exhibit very different amounts of saturation. The Fe II line, on the other hand, reacts quite differently to temperature due to its much higher combined ionisation and excitation energy. Solanki and Pahlke (1988) failed to even remotely reproduce the Stokes V asymmetry of these four lines with 1-D models which were otherwise consistent with observations. This gives me confidence that the δA values of this set of lines are sufficiently sensitive to atmospheric structure to distinguish between at least some models. Although using more lines has its advantages, I have preferred to concentrate on investigating as wide a variety of *model* parameters as possible, leaving the study of more lines to a future investigation.

Table 1. Atomatic data of selected lines

Ion	λ (Å)	χ_e (eV)	$g_{\rm eff}$	$\log g^* f$
Fe I	5083.345	0.96	1.25	−2.958
Fe I	5127.684	0.05	1.0	−6.125
Fe II	5197.574	3.23	0.7	−2.380
Fe I	5250.217	0.12	3.0	−4.938

2.4. *Observational data*

The calculated line parameters are compared with observations obtained near solar disk centre using the Fourier transform spectrometer (FTS) and the McMath telescope in 1979. Stenflo et al. (1984) give a detailed description of the data. The observed values of the relevant line parameters are listed in Table 2. The upper row for each spectral line lists line parameters derived from an active region plage, while the lower row lists data obtained in an enhanced network element. The exception to this rule are the solar wavelength, $\lambda_\odot$ (from Pierce and Breckinridge, 1973), and the Stokes I equivalent width, $W_\lambda(I)$ (from Solanki and Steenbock, 1988), for which quiet sun values are given. δA is the relative area asymmetry of Stokes V, $\delta a/\delta A$ is the ratio of relative amplitude asymmetry to δA, a_b and A_b are, respectively, the unsigned amplitude and unsigned area of the blue Stokes V wing. $v_D(I_V)$, the half width of the I_V or integrated V profile, is a measure of the width of Stokes V. Throughout this paper, the half width of a line profile is defined following Stenflo and Lindegren (1977), i.e. it is given by the Doppler width of a Gaussian which has the same width at half minimum as the line profile. In a 1-D 2-component model I_V can be interpreted as an approximation to the Stokes I profiles formed inside the magnetic feature. It has the advantage that it can be parameterised in exactly the same way as Stokes I (cf. Solanki and Stenflo, 1984, 1985). The I_V width correlates well to the wavelength difference between the blue and red Stokes V peaks, an alternative parameter for describing the width of Stokes V. In the last column of Table 2 $W_\lambda(I_V)$, the equivalent width of the I_V profile, normalised to an average field of 100 G, is listed. This normalisation does not affect the $W_\lambda(I_V)$ of one line relative to another in a given region and also leaves trends with the temperature etc. unaltered. The Stokes V zero-crossing wavelength of the individual lines has not been listed. Solanki (1986) was able to set an upper limit of $\pm 250\ \mathrm{m\,s^{-1}}$ on any such shifts. Note, that the error bars given in Table 2 refer only to the statistical error and in some cases the uncertainties may be larger due to other factors, e.g. blends (cf. Sánchez Almeida et al., 1989).

Noise is a problem when determining δa and δA of Fe I 5127.7 Å. The line profile itself looks quite symmetrical in the plage data (cf. Fig. 3 of Solanki and Pahlke, 1988), but is unusable in the network data. Note also that $\delta a/\delta A$ can vary considerably from one line to another, but tends to be $\gtrsim 2$ for the three stronger lines for which reliable values are available. The asymmetry values of the chosen spectral lines are roughly representative of other lines of similar strength and excitation potential. The amplitude and area of the blue Stokes V wing, a_b and A_b, listed in Table 2 have been scaled by a factor of 2 following Stenflo and Harvey (1985). However, this scaling in no way affects the conclusions of the present paper.

3. Results of models with flows outside the magnetic elements only

In this section only those models are considered which have no velocities within the magnetic elements (i.e. $v_{\mathrm{int}} = 0$). Initially, in Sect. 3.1, I consider a basic model which has a constant flow velocity outside the tube (i.e. $v_{\mathrm{ext}} = \mathrm{constant}$), a $T_{\mathrm{ext}}(z) = T_{\mathrm{HSRASP}}(z)$ and a $T_{\mathrm{int}}(z) = T(z)$ of the network flux tube model. Only results for Fe I 5250.2 Å are discussed, but they are analysed in considerable detail to obtain a better insight into the processes involved in producing asymmetric Stokes V profiles within the context of a 2-D model. Later, in Sect. 3.2, some unsuccessful attempts to improve the match to the data by changing various model parameters and assumptions are described. Finally, in Sect. 3.3 I present the results of model calculations with various T_{ext} which enhance the fit to the data.

3.1. *Results of the basic model*

Figure 1 shows various Stokes V line parameters of Fe I 5250.2 Å calculated with the basic model. In Fig. 1a the relative area asymmetry δA, and in Fig. 1b the relative amplitude asymmetry δa are plotted vs. radius r. The δA and δa values plotted at a given r belong to the area weighted mean Stokes V of all the profiles formed along rays between the flux tube axis and r. The scale of the horizontal axis can be set arbitrarily, since, for the thin tube approximation, the true diameter of the magnetic element is irrelevant for the resulting line profiles. I have chosen to set $r = 1$ at the point where the canopy starts for Fe I 5250.2 Å, so that $\delta A = 0$ for $r < 1$. To help compare the results of the present model with the generally used two-component model I introduce the filling factor, α, which denotes the fraction of the local solar surface covered by the magnetic field *at a given height in the atmosphere*. Here this height is taken to be just slightly above $\tau = 1$ in the flux tube. The horizontal axis (for $r > 1$) can then also be

Table 2. Observed Stokes I and V parameters

Ion	$\lambda_\odot$ (Å)	δA (%)	$\delta a/\delta A$	a_b	A_b (Å)	$v_D(I_V)$ (km s^{-1})	$W_\lambda(I)$ (mÅ)	$W_\lambda(I_V)$ (mÅ/100G)
Fe I	5083.345	5.35 ± 0.84	3.64 ± 0.62	6.6×10^{-2}	3.6×10^{-3}	4.36	111.0	140.2
		6.79 ± 2.05	3.49 ± 1.06	1.5×10^{-2}	8.8×10^{-4}	4.12		33.6
Fe I	5127.684	-2.06 ± 4.14	-1.79 ± 4.98	6.0×10^{-3}	2.7×10^{-4}	2.37	14.3	7.7
		24.20 ± 22.38	1.04 ± 1.17	1.3×10^{-3}	4.4×10^{-5}	1.93		0.8
Fe II	5197.574	4.43 ± 0.97	4.17 ± 0.98	3.5×10^{-2}	1.9×10^{-3}	4.06	79.0	133.8
		4.50 ± 3.52	6.67 ± 4.32	8.2×10^{-3}	4.6×10^{-4}	4.29		32.9
Fe I	5250.217	5.21 ± 0.42	1.84 ± 0.22	6.5×10^{-2}	4.4×10^{-3}	3.85	65.0	62.1
		8.21 ± 1.91	2.35 ± 0.56	1.3×10^{-2}	8.6×10^{-4}	3.80		11.8

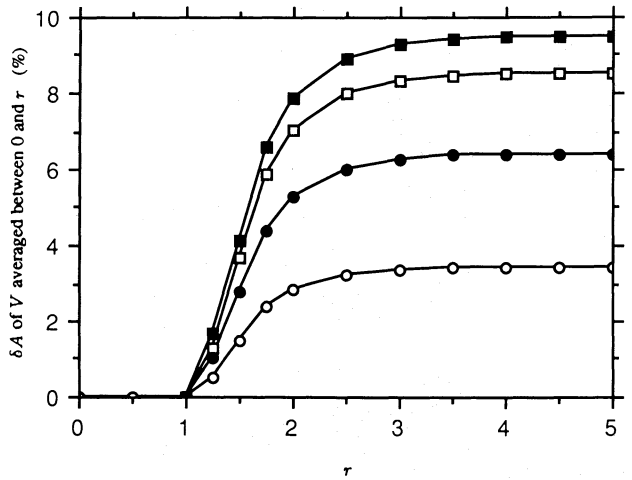

Fig. 1a. Relative area asymmetry, δA, of Fe I 5250.2 Å in % vs. r, the distance from the axis of the flux tube in units of the radius of the "central cylinder" of the flux tube. The δA values plotted at any given r in the figure belong to the average of the Stokes V profiles formed between the axis of the tube and r. The four curves represent results for the following, height independent, external downflow velocities, $v_{ext}=0.5$ km s^{-1} (open circles), 1 km s^{-1} (filled circles), 1.5 km s^{-1} and 3 km s^{-1} (open squares), and 2 km s^{-1} and 2.5 km s^{-1} (filled squares). The basic model is used, i.e. internal temperature is given by the network model of Solanki (1986), with B ($\tau=1$) = 2000 G, no internal velocity is present and the HSRASP represents the external atmosphere

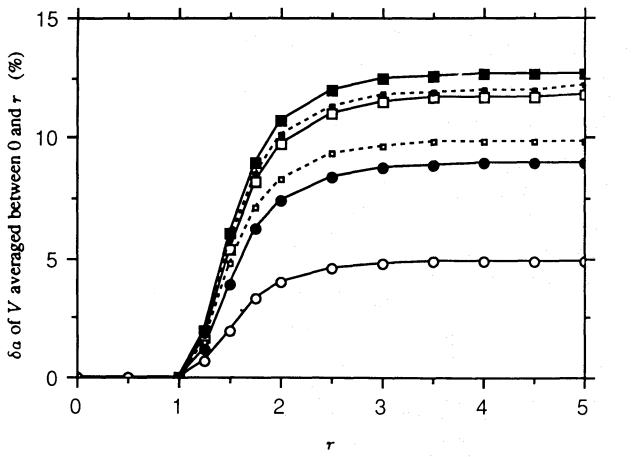

Fig. 1b. Relative amplitude asymmetry, δa, of the averaged Stokes V profiles of Fe I 5250.2 Å in % vs. r for the basic model. The symbols refer to the same v_{ext} as in Fig. 1a. However, now the curves for $v_{ext}=2.5$ km s^{-1} and 3 km s^{-1} are plotted separately (dashed) with smaller symbols to distinguish them from $v_{ext}=2$ km s^{-1} and 1.5 km s^{-1}, respectively

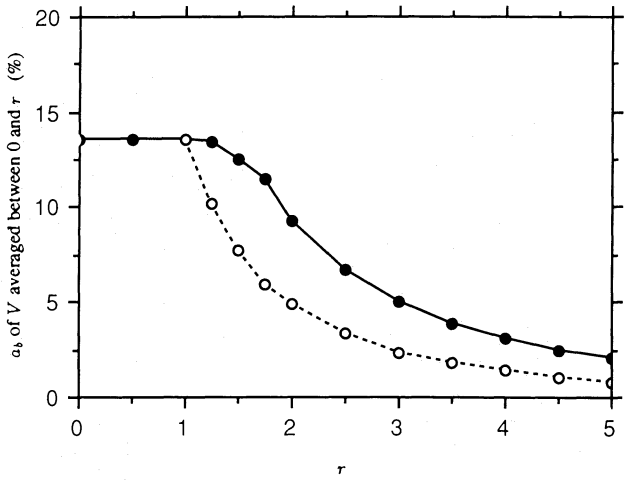

Fig. 2a. a_b, the amplitude of the blue wing of the averaged Stokes V profile of Fe I 5250.2 Å in % vs. r. Solid curve and filled circles: a_b resulting from the 2-D basic model with $v_{ext}=0.5$ km s^{-1}. Dashed curve and open circles: a_b from a 1-D, 2-component model, where the magnetic component is represented by the "central cylinder" of the basic model flux tube and the nonmagnetic component by the HSRASP. The difference between the two curves is mainly due to the contribution from the "canopy" (a small part is due to the different asymmetry of Stokes V

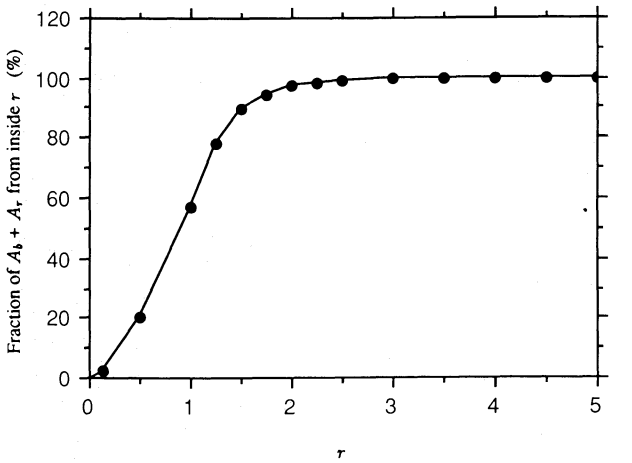

Fig. 2b. Fraction of the summed absolute values of the Stokes V blue and red wing areas, A_b+A_r, coming from inside the radius r for Fe I 5250.2 Å in % vs. r. The Stokes V profiles are weighted according to the area they represent and then added together (without averaging). The basic model is used, with $v_{ext}=1.0$ km s^{-1}. Other values of v_{ext} give almost identical curves

interpreted as representing $1/\sqrt{\alpha}$. As r increases the filling factor (as defined above) must decrease, since the fraction of the surface area covered by the magnetic element at a given height decreases compared to the total surface area within r. Also, with increasing r the Stokes V amplitude decreases, as expected for decreasing filling factor (Fig. 2a).

δA is shown for four values of v_{ext}, namely 0.5 km s^{-1} (open circles), 1.0 km s^{-1} (filled circles), 1.5 km s^{-1} (open squares) and 2.0 km s^{-1} (filled squares). δA values have also been determined for models with $v_{ext}=2.5$ km s^{-1} and $v_{ext}=3.0$ km s^{-1} which give almost the same δA as $v_{ext}=2.0$ km s^{-1} and $v_{ext}=1.5$ km s^{-1}, respectively. Thus, δA increases steadily with v_{ext} up to $v_{ext}\approx 2.25$, but decreases for larger v_{ext}. This suggests that there is a maximum δA of approximately 10% for this line, produced by the basic model, irrespective of the downflow velocity.

Note that 2–2.5 km s^{-1} corresponds to the width of the Stokes V profiles (i.e. the half width of the I_V profiles) formed in the canopy of the flux tube. Thus the present calculations are in agreement with the results of Grossmann-Doerth et al. (1989b), who show that δa and δA are largest when $v_{ext}\approx$ Doppler width of

the line profile for the case when the Zeeman splitting is not too large.

δA also increases with increasing r (i.e. decreasing filling factor). For Fe I 5250.2 Å the main contribution to δA comes in the range of radii between 1 and 2, reaching approximately 80% of the δA value at large r by $r=2$. At a greater distance from the flux tube axis the contribution of any individual ray to Stokes V is extremely small, despite the large area represented by that ray, and δA becomes essentially constant. It is gratifying that even with reasonable values of v_{ext} ($0.5 \lesssim v_{ext} \lesssim 1.5$ km s^{-1}) δA values comparable to the observations are produced, although only the canopy profiles are asymmetric. These results are compatible with unpublished calculations by Van Ballegooijen (private communication).

As can be seen from Fig. 1b, δa shows a qualitatively similar behaviour to δA. For all the calculated cases $\delta a > \delta A$, but the ratio $\delta a/\delta A$ decreases markedly as v_{ext} is increased, being 1.42 for $v_{ext}=0.5$ km s^{-1}, but only 1.17 for $v_{ext}=3.0$ km s^{-1}. The major part of this decrease in $\delta a/\delta A$ occurs above $v_{ext}=1.5$ km s^{-1}. Consequently δa for $v_{ext}=2.5$ and 3.0 km s^{-1} do not coincide with δa for $v_{ext}=2.0$ and 1.5 km s^{-1}, respectively, and are plotted separately in Fig. 1b as the dashed curves (small filled squares: 2.5 km s^{-1}, small open squares: 3.0 km s^{-1}).

Since the δa and δA values increase as the "filling factor" decreases, it would appear at first sight that the model directly predicts an increase in δA and δa with decreasing α. To judge the relevance of this result for the observations, the r corresponding to the observations must be found, which is best done by comparing the amplitude of the blue Stokes V wing, a_b, directly with the observations. In Fig. 2a the a_b resulting from the basic model is represented by the upper curve (plotted solid). As expected, a_b remains constant within the central cylinder and decreases with r in the canopy. The lower curve (dashed) results when the influence of the canopy rays is suppressed, i.e. only the contribution of the central cylinder is retained. As expected, a_b decreases like $1/\alpha$ in this simple two component case. One interesting, but again not too surprising, conclusion which may be drawn from this figure is that in the 2-D case the filling factor (near $\tau=1$), which give rise to a given V amplitude is considerably smaller than in the 1-D case. The observed a_b values may be obtained from Table 2. It follows that for comparison with the network region data the asymptotic values of δA and δa ($r\to\infty$) should be used, while for the active region plage, the slightly smaller values near $r=2.5$ are of interest, although the asymptotic result may also be taken. Any real difference there might be between the asymmetry measured in the two regions cannot be explained directly by the difference in filling factor in this model. Since the observed plage region shows rather strong Stokes V profiles and other signs of a high flux density (compare with Schüssler and Solanki, 1988), this means that the models predict similar δa and δA for all non-sunspot and non-pore magnetic regions, as long as the other atmospheric parameters remain independent of α.

Although they are asymmetric, all the Stokes V profiles calculated in this section, where velocity within the tube is zero, have zero-crossing wavelengths corresponding to their rest wavelengths. This result has been rigorously proved by Grossmann-Doerth et al. (1988, 1989b).

Figure 2b shows the total area of the V profile, A_b+A_r, if all the contributions from the axis of the flux tube out to r are added together, vs. r. The surface area represented by each profile is used as a weight, but the final profiles are not averaged, in contrast to those in Fig. 1. The curve is normalised such that its maximum is exactly 100. These profiles were calculated with $v_{ext}=1$ km s^{-1}, but the curves for other v_{ext} values are practically identical. Approximately 60% of the contribution to the total V profile comes from the central cylinder of the flux tube, suggesting that at solar disk centre for *some* applications 1-D models are a reasonable, but not perfect, approximation. Even if 2-D calculations are carried out, for many purposes it should be quite sufficient to consider no rays from $r>2$ or perhaps even $r>1.5$, since the contribution to A_b+A_r has reached 97%, respectively 90% of the asymptotic value by then for this line. For the asymmetry, however, rays out to at least $r=2.5$ should be considered. For example, at $r=1.5$ both δA and δa of the averaged profile have reached only approximately 40% of their values at large r (Fig. 1).

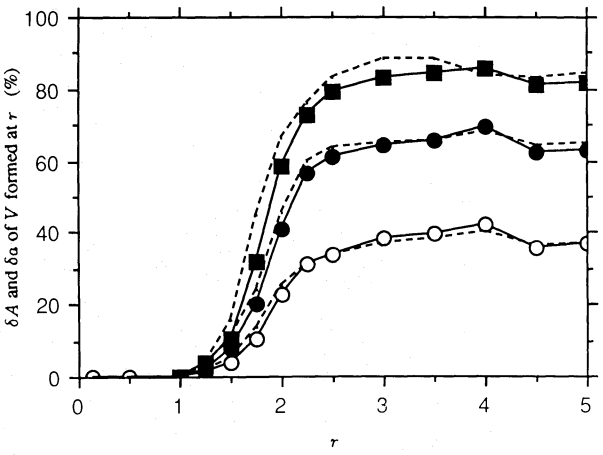

Fig. 3. δA (solid) and δa (dashed) of Fe I 5250.2 Å V profiles formed along the individual rays at distances r from the flux tube axis vs. r. Open Circle: $v_{ext}=0.5$ km s^{-1}, filled circles: $v_{ext}=1$ km s^{-1}, filled squares: $v_{ext}=2$ km s^{-1}. Basic model. For $r\gtrsim 4$ the very small Stokes V profiles ($a_b+a_r \lesssim 10^{-4}$) may be slightly affected by numerical inaccuracies. The small wiggles beyond $r=3.5$ may, therefore, be of numerical origin

Note that unlike Stokes V, which receives more than half of its contribution from the central cyliner irrespective of the filling factor, Stokes I gets an increasingly smaller fraction from there as the filling factor decreases. The Stokes I profiles of Fe I 5250.2 Å formed along individual rays at $r>2$ all are rather similar to the Stokes I profile in the quiet sun, since the canopy boundary is by then so high that the magnetic atmosphere gives little contribution to the I profile. The averaged Stokes I profile, however, differs from the quiet sun line profile even at considerably larger r, due to the still significant contribution of the central cylinder of the flux tube.

The relatively small contribution of the canopy to the averaged Stokes V profile also implies that the Stokes V profiles produced in parts of the canopy must be extremely asymmetric. The contribution of the individual rays (or rather the concentric cylindrical shells they represent) to δA and δa of Stokes V of Fe I 5250.2 Å is illustrated in Fig. 3 (the symbols are the same as in Fig. 1). This figure shows that the individual Stokes V profiles can have δA and δa values of over 80% (for Fe I 5083.3 Å δA values of well over 90% are seen). Such profiles are almost completely composed of only one Stokes V wing. Therefore, a very steep gradient in v and B extending over a short height range (i.e. a jump in these quantities) appears to be more efficient in producing a Stokes V asymmetry than a more gradual change extending

over a larger height. Also, the efficiency of a given jump in magnetic field strength and velocity in producing a Stokes V asymmetry increases with increasing height in the atmosphere. This result is not an artefact of the decrease in field strength with height, since a series of 1-D test calculations with fixed B and v magnitudes, but a varying height at which the jumps in B and v occur, shows precisely the same effect.

Since δA (or δa) cannot become larger than 100%, the averaged Stokes V profile of any line cannot have a δA (or δa) larger than a certain value corresponding to the relative contribution of the "canopy" profiles to the average. In general this contribution depends on the run of the internal and external gas pressure and on the magnetic tension effects (Pneuman et al., 1986; Steiner and Pizzo, 1989), and on the properties of the spectral line. In the model used here this limit corresponds to 30–40%. However, as can be seen from Fig. 1a, this limit is far too conservative for Fe I 5250.2 Å for the basic model. In practice, only δA and δa values well below this limit are expected.

Another interesting feature may not be so readily visible from Figs. 1 and 3. The $\delta a/\delta A$ ratio of the averaged profiles is always larger than of any of the profiles formed along the individual rays. Thus for some of the profiles resulting from individual rays, $\delta a/\delta A$ is smaller than unity, while for all averaged profiles $\delta a/\delta A > 1$. This difference in the $\delta a/\delta A$ ratio is to be attributed to the fact that δa, unlike δA, does not require a velocity gradient *along the line of sight* for its production. For example, if two (or more) antisymmetric Stokes V profiles, which are shifted with respect to each other, are superposed then the resulting profile will also have $\delta A = 0$, but not necessarily $\delta a = 0$. δa can also be enhanced (or diminished) relative to δA if at least one of the superposed Stokes V profiles is already asymmetric, even if the profiles are *not* shifted with respect to each other. The latter is the case when combining the antisymmetric V coming from the central cylinder of the flux tube with the asymmetric profiles from the canopy. The δa value is always enhanced relative to δA in the considered cases (although it is smaller than the δa of most of the canopy profiles alone).

Let me now turn to the width of Stokes V (represented by the half width of the I_V profile, cf. Sect. 2.4). For Fe I 5250.2 Å there is a clear tendency for the width to decrease with increasing r. This has at least partly to do with the larger Zeeman splitting in the central cylinder, because the stronger field strengths in the lower part of the tube are only present there. For the other three lines this decrease in line width is smaller, but is generally still present. However, the more important effect is that *with increasing* v_{ext} the line width consistently shows a small but distinct *decrease* for all four lines. For example, the I_V width of Fe I 5250.2 Å decreases by almost 0.2 km s^{-1} between $v_{ext} = 0$ and 3 km s^{-1}. For a given change in v_{ext} the decrease in line width is larger for stronger lines, suggesting that it is a saturation effect. I shall return to a discussion of line widths in Sect. 3.2.

How do the Stokes V profiles calculated so far compare with observations? Although the observed δA and zero-crossing wavelength of a single Stokes V profile may be reproduced very simply with the "basic"model used so far, the δA of the four chosen lines cannot be reproduced by a single reasonable v_{ext} value. In addition, the calculated $\delta a/\delta A$ ratios for Fe I 5083.3, 5250.2 and Fe II 5197.6 Å are too small, as are the widths of the average Stokes V profiles of all four lines. Obviously the model must be modified if it is to explain the observations quantitatively.

3.2. *Modifications to the basic model*

In this section I briefly describe various attempts to improve the fit to the data. Although they are all unsuccessful, they do provide insight into how the Stokes V asymmetry reacts to changes in the model. Such calculations are necessary before the Stokes V asymmetry can be used as a diagnostic. One modification which is not considered is changing B ($\tau = 1$), since this quantity is rather well determined by the observations. The calculations presented by Grossmann-Doerth et al. (1989) suggest that changing the magnetic field strength within reasonable limits may slightly change the results quantitatively, but not qualitatively. Unless otherwise stated, the results considered from now on (i.e. in Sects. 3.2, 3.3 and 4) are derived from Stokes V profiles averaged between $r = 0$ and $r = 4$. The results are not expected to depend significantly on the outer boundary for the averaging as long as it is larger than $r = 2.5$ (cf. Figs. 1 and 2).

As the first modification I let v_{ext} have a vertical gradient, i.e. a linear vertical velocity profile is chosen throughout the non-magnetic atmosphere. This modification is unable to bring the δA values of Fe I 5083.3, 5250.2 and Fe II 5197.6 Å significantly closer together. It appears that the flanks of the four lines used here are either not formed sufficiently far apart in the atmosphere for them to see very different velocities, or the velocity gradients considered here are too small. The largest velocity gradient I have tried gives $|v_{ext}(\tau = 1) - v_{ext}(\tau = 10^{-4})| \approx 5$ km s^{-1}. However, note that since the asymmetry is produced almost exclusively in a relatively thin ring round the flux tube (two thirds of the total δA are produced within a height range of 100 km), the vertical velocity gradient would have to be very large indeed to show a sizeable effect. The line widths and the $\delta a/\delta A$ ratios are not increased by this measure either.

A similar modification is to introduce a "boundary layer" around the flux tube, such that far from the flux tube boundary the flow velocity remains constant, but closer to the flux tube it decreases linearly towards the boundary. There are physical reasons for expecting the presence of a boundary layer, e.g. the finite viscosity of the solar gas. Some models have also been calculated in which the velocity remains zero out to a certain distance from the flux tube boundary before assuming a constant non-zero value. Neither modification solves any of the outstanding problems, but the results are instructive from a general point of view. They show to what distance from the flux tube boundary the sensitivity of the Stokes V profile to velocity extends. Obviously, the broader the zero-velocity region around the flux tube, the smaller are the δA and δa produced. Any variation in the velocity farther away from the boundary than the width of the contribution function of the V profile is not felt at all. Also, a steep gradient in v_{ext} close to the boundary, but leveling off to a relatively small constant value of v_{ext} gives a similar δA as a v_{ext} with a small initial gradient but a larger final constant value.

Next, I have changed the geometry of the model flux tube by considering a flux slab instead. The main differences for the model calculations are that the "diameter" (or rather width) of the slab increases as $1/B$ (instead of $1/\sqrt{B}$ for the tube) and the individual rays now all have the same weight. The results are similar to those of the cylindrical case. None of the problems present with the original model are removed or reduced. For the rest of this paper I, therefore, revert to the cylindrical flux tube model.

Another possibility is based on the fact that $\delta a/\delta A$ of the profiles formed along individual rays varies (for a constant v_{ext})

with r. Therefore, one way of increasing $\delta a/\delta A$ of the averaged Stokes V profile may be to concentrate the downflows into a thin cylinder around the flux tube (i.e. a small range of r values), where $\delta a/\delta A$ is maximal. One problem with this approach is that the dependence of $\delta a/\delta A$ on r is itself a function of various parameters. Although it is more common for $\delta a/\delta A$ to decrease with increasing radius, the opposite dependence is also observed. It is difficult to obtain $\delta a/\delta A > 2$ in this manner, and I have been unable to achieve values greater than 2.5, as are observed for e.g. Fe I 5083.3 and Fe II 5197.6 Å. One reason for the failure of this attempt at a solution may be that if the downflow is concentrated into a thin ring, then the flow must be stronger and locally Stokes V must have a δA value approaching 100% to compensate for the smaller fractions of light which results in asymmetric Stokes V profiles. However, since δa also cannot be greater than 100%, the $\delta a/\delta A$ ratio for these profiles then approaches unity again and the advantage is lost. Even the fact that summing the profiles from the central cylinder and the canopy generally enhances $\delta a/\delta A$ cannot compensate for this loss.

A further question one can ask is: Can velocities outside the magnetic element explain the non-thermal, non-magnetic broadening of Stokes V profiles observed by Solanki (1986) and Pantellini et al. (1988)? To answer this question I have also calculated some models with an upflow in the surroundings of the magnetic elements and added the averaged profiles from the upflowing and downflowing models together. Although Stokes I resulting from this procedure is strongly broadened, the Stokes V width is left practically unchanged. For example, if $v_{ext} = \pm 2\ km\ s^{-1}$, then the width of Stokes I of Fe I 5250.2 Å is almost doubled, while the width of Stokes V remains constant to within $20\ m\ s^{-1}$. Therefore, *velocities and velocity gradients outside magnetic features cannot broaden Stokes V profiles.* The non-thermal, non-magnetic line broadening of the Stokes V profiles must have another source, the most obvious candidate being velocities within the magnetic elements. To check whether the $\delta a/\delta A$ value is affected by the combination of external up- and downflow I have also given different weights to the V profile resulting from the model having $v_{ext} < 0$ with respect to the V profile from the model with $v_{ext} > 0$. $\delta a/\delta A$ remains practically unchanged.

As another test the temperature inside the magnetic elements is changed. First, instead of the network model, the slightly cooler plage model of Solanki (1986) is used. Due to the small temperature difference between the plage and network models the influence on δA is small and no principle difference is found to the original δA. Next, models with temperature structures parallel to that of the HSRASP, as described in Sect. 2.1, are used. Figure 4 shows δA of Fe I 5083.3 Å (squares) and 5250.2 Å (diamonds) vs. ΔT_{int} for $v_{ext} = 1\ km\ s^{-1}$. $\Delta T_{int} = 0$ corresponds to the HSRASP temperature structure. δA of both lines increases rapidly with decreasing temperature over the complete temperature range. δA of 5083.3 Å always remains significantly larger than that of 5250.2 Å, which is contrary to the observations.

The basic reason for the behaviour of δA exhibited in Fig. 4 is the strengthening of the spectral lines inside the flux tube with decreasing ΔT_{int}. As pointed out by e.g. Solanki and Pahlke (1988), the associated increase in saturation produces a larger asymmetry. Thus, $W\lambda$ (I_V), the equivalent width of the I_V profile (I_V is the integrated V profile, cf. Sect. 2.4), changes between 38.1 mÅ $(100\ G)^{-1}$ at $\Delta T_{int} = +600$ K and 247.3 mÅ $(100\ G)^{-1}$ at

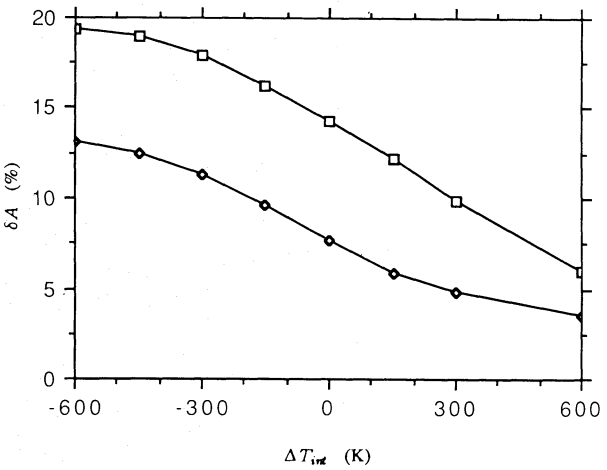

Fig. 4. δA (in %) of the Fe I 5083.3 Å (squares) and 5250.2 Å (diamonds) V profiles averaged between $r = 0$ and 4, vs. ΔT_{int}, the difference between the temperature inside the magnetic element and the HSRASP. $\Delta T_{int} < 0$ signifies that the magnetic element is cooler than the average quiet sun. The external atmosphere is given by the HSRASP and $v_{ext} = 1\ km\ s^{-1}$. $B(\tau = 1) = 2000$ G and no internal velocity is present

-600 K for Fe I 5250.2 Å. W_λ (I_V) of Fe I 5083.3 Å varies by a similar amount.

δa exhibits a similar behaviour to δA and no clear trend is seen in $\delta a/\delta A$. In particular, no $\delta a/\delta A$ values greater than 1.8 are observed, which is clearly inadequate to explain the observed $\delta a/\delta A$ of e.g. 5083.3 Å. In addition, a change in temperature within the flux tube has a very strong influence on the ratios of the Stokes V wing areas of one line to another. Such ratios are used to diagnose the temperature within solar magnetic elements and their observed values set relatively narrow limits on ΔT_{int}. In summary, this modification is, like the others before it, unable to overcome the existing problems.

3.3. *Modification of the temperature in the surroundings*

In this section I study the effect of changing the temperature of the surroundings of the model flux tube in the manner described in Sect. 2.1. A series of models with ΔT_{ext} values ranging from -600 K to $+300$ K are calculated. ΔT_{ext} is zero for the temperature structure of the HSRASP. The resulting δA of all four lines are plotted as a function of ΔT_{ext} in Fig. 5a for $v_{ext} = 1\ km\ s^{-1}$ (Fe I 5083.3 Å: open squares, Fe I 5127.7 Å: solid diamonds, Fe II 5197.6 Å: solid squares, Fe I 5250.2 Å: open diamonds). δA of each of the lines has a distinctive dependence on ΔT_{ext}. The most interesting point is near $\Delta T_{ext} = -300$ K. There Fe I 5083.3, 5250.2 and Fe II 5197.6 Å have relatively similar δA values, in accordance with the observations. Therefore, it is possible to remove one of the main shortcomings of the current model with this measure, and it is worth looking at the influence of ΔT_{ext} on these lines in greater detail.

A change in ΔT_{ext} mainly affects the level populations in the non-magnetic part of the atmosphere and thus the strengths of the Stokes I profiles formed there. Since the amount of saturation in the spectral profiles entering the tube is one of the strongest factors influencing δA and δa, it is natural that these parameters are also strongly affected by ΔT_{ext}. As it is not so straightforward

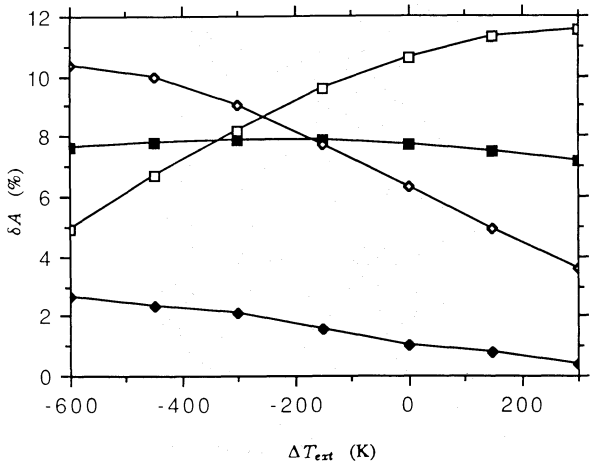

Fig. 5a. δA in % of V profiles averaged between $r=0$ and 4 of Fe I 5083.3 Å (open squares), 5127.7 Å (filled diamonds), Fe II 5197.6 Å (filled squares) and Fe I 5250.2 Å (open diamonds) vs. ΔT_{ext}, the temperature difference between the non-magnetic atmosphere surrounding the magnetic elements and the HSRASP. $v_{ext}=1\ km\ s^{-1}$, the network flux tube model with $B\ (\tau=1)=2000$ G represents the atmosphere inside the flux tube

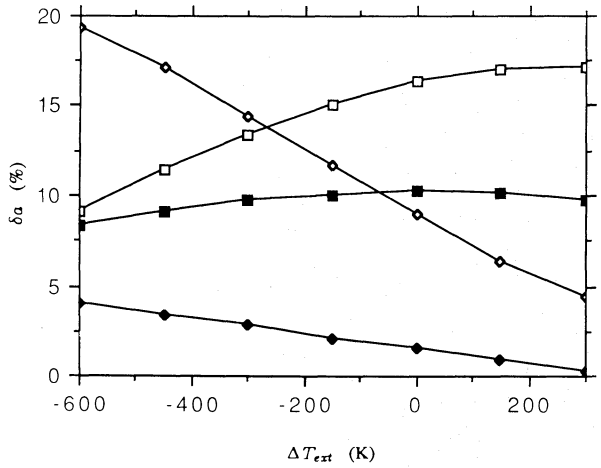

Fig. 5b. δa in % of the same Stokes V profiles are represented in Fig. 5a (denoted by the same symbols) vs. ΔT_{ext}

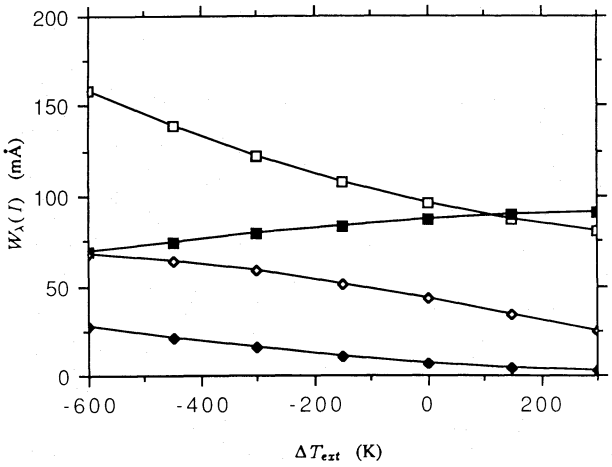

Fig. 6a. The equivalent width of the Stokes I profiles, $W_\lambda\ (I)$, in mÅ vs. ΔT_{ext}. The same line profiles are represented as in Fig. 5a

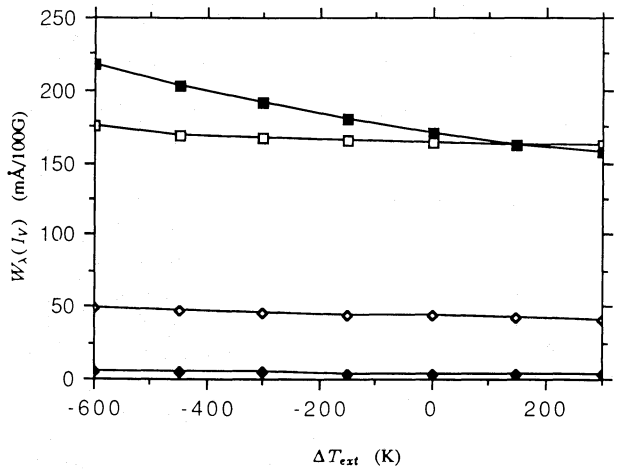

Fig. 6b. The equivalent width of the I_V or integrated V profile, $W_\lambda(I_V)$, in mÅ, normalised to an average field of 100 G vs. ΔT_{ext}. The same line profiles are represented as in Fig. 5a

to analyse the profile entering the flux tube canopy, I have settled for plotting the emergent Stokes I, which gets its main contribution from outside the tube under the canopy (due to the higher gas density and generally lower temperature and correspondingly higher neutral iron level populations there).

Figure 5b shows δa vs. ΔT_{ext}. The similarity to Fig. 5a is evident and suggests that $\delta a/\delta A$ is not significantly affected by changing ΔT_{ext}. It remains smaller than two for all four lines and the considered temperatures.

In Fig. 6a W_λ is plotted as a function of ΔT_{ext}. δA correlates only partially with $W_\lambda\ (I)$ of the average Stokes I profiles. Whereas δA increases rapidly with increasing $W_\lambda\ (I)$ for $W_\lambda\ (I) \lesssim 70$ mA, it decreases again as $W_\lambda\ (I)$ increases beyond this value. A qualitatively similar effect has previously been suspected by Skumanich and Lites (1987) and has been quantified by Sánchez Almeida et al. (1989) in the framework of analytical solutions of special cases of the transfer equations for polarized light (magnetic field parallel to the line of sight, Milne-Eddington atmosphere). It is also in general agreement with the observations (e.g. Solanki and Stenflo, 1984; Pantellini et al., 1988). A heuristic explanation of the qualitative behaviour of δA as a function of W_λ has been given by Grossmann-Doerth et al. (1989b). The behaviour is due to the line width which, for sufficiently large W_λ, increases rapidly with increasing W_λ, while the saturation in the line flanks (where Stokes V is maximal) remains essentially unchanged. Since the relation between line width and line strength is somewhat different for the four lines (due to different g_{eff} values, damping constants and heights of formation), the relation between δA and $W_\lambda\ (I)$ is also not unique, although similar.

Keeping the above change in the trend of δA vs. $W_\lambda\ (I)$ in mind, the behaviour of δA of the four lines can be easily understood as a consequence of their respective oscillator strengths and excitation

potentials. Fe I 5127.7 is a very weak line showing practically no saturation at $\Delta T = +300$ K and consequently having practically no δA or δa either. As ΔT_{ext} decreases this low excitation line becomes stronger and its δA and δa increase proportionally. Fe I 5250.2 Å is stronger (larger log gf), thus having a larger δA at all ΔT_{ext} values, but shows a behaviour qualitatively similar to Fe I 5127.7 Å, it also being a low excitation line. The Fe II line at 5197.6 Å, being relatively temperature independent, has a δA and δa which are not greatly affected by ΔT_{ext}. Furthermore, its $W_\lambda(I)$ varies in a range where the change in sign of the dependence of δA on W_λ takes place is it being somewhat stronger than Fe I 5250.2 Å. Finally, as expected for a strong low excitation line, Fe I 5083.3 Å shows a decreasing δA and δa but an increasing $W_\lambda(I)$ with decreasing ΔT_{ext}.

Although ΔT_{ext} strongly affects the equivalent width of Stokes I, its influence on Stokes V, rather small. This is illustrated in Fig. 6b, where the equivalent width of the I_V profile, $W_\lambda(I_V)$, is plotted vs. ΔT_{ext}. The I_V profile has been arbitrarily normalised to an average field of 100 G. Consider, for example, the highly temperature sensitive line Fe I 5127.7 Å. The equivalent width of its Stokes I changes by a factor of approximately 10 between $\Delta T = +300$ K and -600 K, while $W_\lambda(I_V)$ changes by less than 30%. Only the Fe II lines may be considered an exception to this rule. The reason for its anomalous behaviour is not understood. Other temperature sensitive Stokes V parameters (e.g. $A_b + A_r$ and $a_b + a_r$) are also only slightly affected by ΔT_{ext}. In general, *at solar disk centre, if its asymmetry is ignored, the Stokes V profile is mainly sensitive to conditions within the magnetic features*, even if many lines of sight pass partly through both the magnetic and non-magnetic parts of the atmosphere. However, Stokes V is not completely insensitive to the external atmosphere and future 2-D empirical models of magnetic elements based on Stokes V profiles will have to take this effect into account. There are two reasons for the relative insensitivity of Stokes V to T_{ext} (excluding the V asymmetry). Firstly, Stokes V feels the external temperature only through saturation effects. The Stokes V profile does not directly react to changes in the level populations outside the magnetic element in LTE. Secondly, as can be seen from Fig. 2b, for any filling factor more than half of the contribution to the Stokes V profile averaged over the whole magnetic element comes from the central cylinder of the flux tube and, in LTE, does not feel the conditions in the non-magnetic atmosphere at all. This dilutes any effect of the external atmosphere on the averaged profile.

A comparison of Fig. 4 with Fig. 5a leads to the question why e.g. δA of Fe I 5083.3 Å behaves so differently in the two figures. In particular, why does δA keep increasing as ΔT_{int} is decreased, right down to $\Delta T_{int} = -600$ K? One reason for the difference is that the variation in $W_\lambda(I)$ for a given change in T_{int} is smaller than for the same change in T_{ext}. However, the line shape must also play a role, because the $W_\lambda(I)$ partly overlap in the two series of test calculations and even in these overlapping ranges the dependence of δA on $W_\lambda(I)$ is quite different. A change in T_{int} mainly affects the line core of the profiles formed in the canopy, since only the upper part of the atmosphere is changed, and conversely when T_{ext} is varied it is mainly the line wings which are affected. Consequently $v_D(I)$, the Stokes I line width at half minimum increases rapidly with decreasing T_{ext}, but much more slowly with T_{int}. The effect on the profile shapes produced by varying T_{int} (solid curves) and T_{ext} (dashed curves) is illustrated in Fig. 7, where $v_D(I)$ is plotted vs. $W_\lambda(I)$ for Fe I 5083.3 Å (squares) and 5250.2 Å (diamonds). This figure actually underestimates the

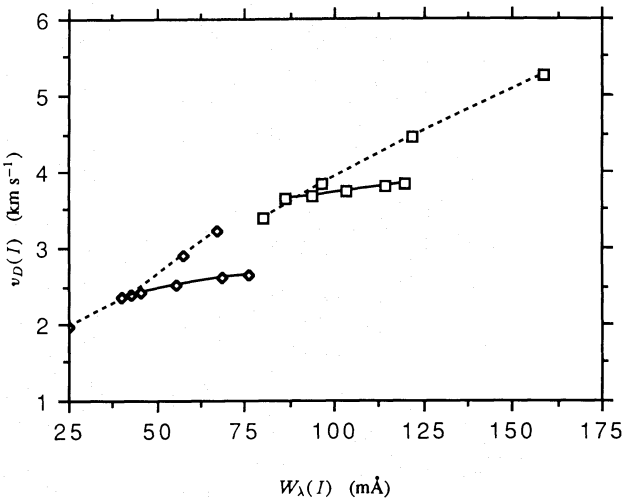

Fig. 7. The width at half minimum of the Stokes I profile, $v_D(I)$, in km s^{-1} expressed as the Doppler width of a Gaussian having the same half-width as the line, vs. $W_\lambda(I)$ in mÅ. Fe I 5250.2 Å is represented by diamonds, Fe I 5083.3 Å by squares. The curves produced by varying ΔT_{ext} are plotted dashed, those resulting from a variation of ΔT_{int} are drawn solid. To enhance clarity symbols have not been plotted at all the calculated points

difference in profile shapes, since it also includes profiles from the central cylinder, which are the same for both series of calculations. Canopy profiles are (generally) narrower in the T_{int} series, than in the T_{ext} series. More importantly, their width remains almost unaffected by ΔT_{int}, so that the main mechanism for causing δA to decrease with increasing $W_\lambda(I)$ does not come into play. Thus, the difference between Figs. 4 and 5a is in line with the heuristic explanation of the δA (W_λ) dependence given by Grossmann-Doerth et al. (1989b).

Let me now turn to a comparison with the data. First, for all ΔT_{ext} values tried, the δA values of the three strong lines lie much closer to each other, and thus closer to the observations, than for the 1-D calculations of Pahlke and Solanki (1986) and Solanki and Pahlke (1988). One reason for this improvement is that in the 2-D model the amount of saturation in the surroundings also decides the asymmetry. Another reason may have to do with the abrupt changes in B and v in the present model, compared to the more gradual gradients used in the previous investigations. The best fit of δA of all four lines to the data (within the observational uncertainty) is obtained for ΔT_{ext} between approximately -250 K and -350 K, i.e. when the surroundings of the magnetic elements are rather cool compared to the average quiet sun. This agrees well with the picture that magnetic elements are mainly found in dark intergranular lanes (Dunn and Zirker, 1974; Mehltretter, 1974; Muller, 1983; Title et al., 1987). Since the amplitudes or wing areas of Stokes V are only slightly affected by changes in T_{ext}, the temperature diagnostics based on Stokes V are not strongly affected by T_{ext}. Even if T_{int} is changed slightly to better reproduce such diagnostics, δA of one line relative to another is hardly affected (cf. Fig. 4) and the results of this section should remain valid. Thus, lowering the external temperature has solved one of the outstanding problems. Additionally, the δA values of multiple lines provide a relatively sensitive diagnostic of the temperature and flow velocity in the surroundings of magnetic elements. Its value is enhanced if traditional Stokes V based

temperature diagnostics (e.g. ratios of amplitudes or wing areas of lines of different temperature sensitivity) are used to set some constraints on the internal temperature.

When deriving ΔT_{ext} it is generally not sufficient to limit the calculations to a single v_{ext} value, as I have done so far, since the form of the δA vs. T_{ext} curve of a given line also depends on v_{ext}. Consequently I have repeated the ΔT_{ext} series of calculations using different v_{ext} and find that v_{ext} derived from the present model for the plage data lies between $0.5-1.0\,km\,s^{-1}$. Calculations using $v_{ext}=0.5\,km\,s^{-1}$ show quite a similar behaviour of δA as a function of T_{ext} as for $v_{ext}=1.0$. In particular, the data are also best reproduced for $-350\lesssim\Delta T_{ext}\lesssim-250$ K.

As pointed out by Solanki and Pahlke (1988), one problem with 1-D models is that, on the one hand, the observed asymmetry tends to be slightly larger in the network, while on the other hand, the higher temperature derived for network magnetic elements (e.g. Solanki, 1986; Keller, 1988) means that Fe I lines calculated for the network are less saturated and therefore in general considerably less asymmetric. This problem is greatly mitigated in the present 2-D model, since the temperature outside the magnetic elements now plays an important role. However, a larger δA in the network still implies that the downflow velocity around the network elements is larger than around the plage elements ($1.0-1.5\,km\,s^{-1}$).

This conclusion does not necessarily contradict the observations of Brandt and Solanki (1989), who note that the parts of the Stokes I line bisectors near the continuum are more redshifted in regions with larger magnetic filling factors. For example, if the granular downflow is enhanced by the presence of magnetic features (e.g. by an additional baroclinic flow around the magnetic elements, as predicted by Deinzer et al., 1984b), then the 3–4 times larger filling factor in the active region implies that Stokes I observations there will see much more of the enhanced downflow than in the network. Even a simple decrease in the temperature contrast between granule centres and the intergranular lanes (abnormal granulation, Dunn and Zirker, 1974) can readily explain the Stokes I line bisector observations, without affecting the Stokes V results. This is an example of how Stokes I and V differ in their diagnostic content, since they sample the light produced in an active region quite differently. Therefore, the combined study of Stokes I and V asymmetry may provide more information on the interaction of the magnetic field with convection, than may otherwise be obtainable.

4. Results of models with velocities inside and outside the magnetic elements

The model constructed so far has had some marked success: It can reproduce the δA and zero-crossing wavelengths of lines with widely different properties using a physically plausible magnetic structure and reasonable values for B, T_{int}, T_{ext} and v_{ext}. But two problems remain. The calculated Stokes V width and the $\delta a/\delta A$ ratio are both too small as compared to the observations. The most obvious remaining extension of the model is the introduction of non-stationary mass motions within the magnetic elements. These are a means of broadening the Stokes V profiles and should resolve at least one of the problems. In addition, there is observational evidence for the notion that internal motions may be responsible for a considerable fraction of δa. From an analysis of observed profiles Solanki (1985, 1986) found a strong correlation between Stokes V broadening velocity and the absolute amplitude asymmetry, a_b-a_r, suggesting an at least partially common cause for δa and Stokes V width. The investigation of the influence of such motions on the Stokes V asymmetry in combination with motions outside the magnetic elements is the subject of the present section. Throughout it only models with $\Delta T_{ext}=-300$ K are considered, in agreement with the results of Sect. 3.

4.1. Models incorporating micro- and macroturbulence

Until now the influence of non-stationary mass-motions on Stokes V profiles has generally been modelled by broadening the calculated profiles with a mactoturbulence velocity distribution, or a combination of macro- and microturbulence (e.g. Solanki, 1986; Solanki et al., 1987; Lites et al., 1988). Although this is a highly idealised approximation and the physical interpretation of a macroturbulence broadening of Stokes V in a 2-D model is unclear, to say the least, it has been successful in reproducing the observed line widths in 1-D models. Therefore, I have convoluted the calculated Stokes V profiles with various Gaussian macroturbulence distributions, here denoted by their e-folding width, the macroturbulence velocity ξ_{mac}. Various values of the microturbulence ξ_{mic} both inside and outside the tube have also been tried.

As expected, the Stokes V widths increase with increasing turbulence velocity and can be made to reproduce the data arbitrarily accurately by convoluting each line with a macroturbulent velocity of the appropriate magnitude. The influnce on the Stokes V asymmetry has already been discussed in detail by Solanki and Stenflo (1986), since a Gaussian macroturbulent velocity distribution acts in formally the same manner as broadening by a Gaussian instrumental profile of the same width. As their results show, with increasing ξ_{mac} δA increases, $\delta a/\delta A$ decreases (for ξ_{mac} values which do not produce too broad V profiles) and the zero-crossing wavelength is shifted increasingly towards the red. A simple macroturbulence alone improves the fit to the line width, but worsens it to the $\delta a/\delta A$ ratio and must, therefore, be rejected.

In general, increasing ξ_{mic} strongly reduces δA and δa. Since ξ_{mic} mainly broadens the line profile, this counts as further support for the result of Grossmann-Doerth et al. (1989b) that δA for weakly Zeeman split lines decreases when the line width becomes large compared to the velocity induced shift of the absorption coefficients. Also, the microturbulence outside the magnetic elements appears to have a larger effect on the Stokes V asymmetry than the ξ_{mic} inside. This can be explained by recalling that ξ_{mic} outside the magnetic element mainly broadens the line flanks, where Stokes V is largest, while the internal ξ_{mic} mainly affects the line core. Values of ξ_{mic} which result in realistic widths of Stokes V profiles (i.e. $\xi_{mic}\lesssim3.0\,km\,s^{-1}$) cannot improve the correspondence of $\delta a/\delta A$ to the observations.

The inability of ξ_{mic} and ξ_{mac} to improve the correspondence with the data suggests that not all of the non-thermal, non-magnetic broadening of Stokes V observed outside sunspots can be truly turbulent in nature.

4.2. A simple oscillatory or wave-like model

In a next step I have constructed a very simple two time-component model of a flux tube wave or oscillation, whose basics are described in Sect. 2.1. For the calculation of the line profiles

the same atmosphere is used in both phases. However, when adding the two phases together to produce the time-averaged Stokes V (which is the proper Stokes V profile to compare with time averaged or low spatial resolution data), the profiles resulting from the two phases can be weighted differently to reflect, in a crude manner, e.g. differences in thermal structure between the upflowing and downflowing phases. Such differences could arise through, for example, radiative damping of longitudinal tube waves or overstable oscillations (e.g. Webb and Roberts, 1980; Hasan, 1985). The extreme case when the weight of one of the phases becomes zero corresponds to a pure stationary up- or downflow. The approach outlined above is not self-consistent. It would be physically more realistic to keep the weights of both components fixed and instead vary their temperatures, but this would increase the computational requirements by an order of magnitude. Since a more comprehensive treatment of flux tube waves involving the solution of the linearised MHD equations is currently underway, no strong reason for this additional complication is felt.

Although this model is primitive, it does contain some of the main features of the influence of waves on Stokes V profiles in flux tubes. Note also that the two components (or phases) of the present simple model need not reflect two different times, although for simplicity this will generally be assumed in the present paper. Since many magnetic elements are present within the resolution element of the FTS observations, the model can also be interpreted in terms of two different flux tubes, one harbouring a stationary upflow, the other a stationary downflow. On average the total mass flux must be close to zero in reality. This condition is fulfilled by e.g., siphon flows (Hasan and Schüssler, 1985; Thomas, 1988; Montesinos and Thomas, 1989).

In the rest of this section I investigate the influence on Stokes V of such "two component waves" in the flux tube with different velocity amplitudes and with different weightings of the up- and downflow phases. These waves are considered on their own and in combination with downflows outside the flux tube. As pointed out in Sect. 3.1, adding two unequally weighted and shifted Stokes V profiles can easily produce a resulting Stokes V profile with a significant δa, even if both the original profiles are antisymmetric. The type of calculations presented in this section should therefore influence δa considerably. However, introducing a velocity in the tube (even a velocity independent of height) generally also leads to the creation of an area asymmetry of Stokes V, due to the presence of the jump in B and $v_{\rm int}$ at the boundary of the flux tube canopy. In contrast to the case of an external flow, for an internal velocity $\delta A>0$ is produced by an upflow (cf., e.g., Eq. (2) of Solanki and Pahlke, 1988) and the Stokes V zero-crossing wavelength is shifted. When an external downflow is also present then it is the difference between the two velocities which is responsible for δA and a part of δa.

Some of the results are illustrated in Figs. 8, 9 and 10. In Fig. 8a the ratio $\delta a/\delta A$ of Fe I 5250.2 Å is plotted vs. the weight, w_u, given to the Stokes V profile resulting from the upflow phase. w_u is normalised such that the sum of the weights of both phases is always unity. For the four curves plotted in the figure the "wave amplitude" is kept fixed at 1 km s^{-1}, i.e. $v_{\rm int}=\pm 1$ km s^{-1}, while $v_{\rm ext}$ varies, being 0.0 km s^{-1} (squares), 0.5 km s^{-1} (triangles), 1.0 km s^{-1} (circles) and 1.5 km s^{-1} (diamonds), respectively. The curves have only been plotted for those values of w_u for which $\delta a/\delta A\geq 0$ and $\delta A>0$. As can be seen, all $\delta a/\delta A$ values below approximately 2.7 can be produced with this $v_{\rm int}$. The $\delta a/\delta A$ variation can easily be understood. Since a height independent $v_{\rm int}$ has been chosen, only the canopy rays give a contribution to the δA of the averaged Stokes V profile, whereas the profiles formed along all rays contribute to the average δa for $w_u\neq 0$, 1. Therefore the influence of the "wave" on δa is considerably larger than on δA, so that the $\delta a/\delta A$ ratio of the spatially and temporally averaged Stokes V profile can be strongly altered. Fig. 8b shows the same parameters as Fig. 8a for Fe I 5083.3 Å. Both lines show qualitatively the same behaviour, although $\delta a/\delta A$ of Fe I 5083.3 Å can be enhanced much more than of Fe I 5250.2 Å, in general agreement with the data. Interestingly, the larger $\delta a/\delta A$ values are always produced when the upflow component is more strongly weighted.

The observations lie between the two horizontal dashed lines. For the illustrated $v_{\rm int}$ the calculations fall into this area only for

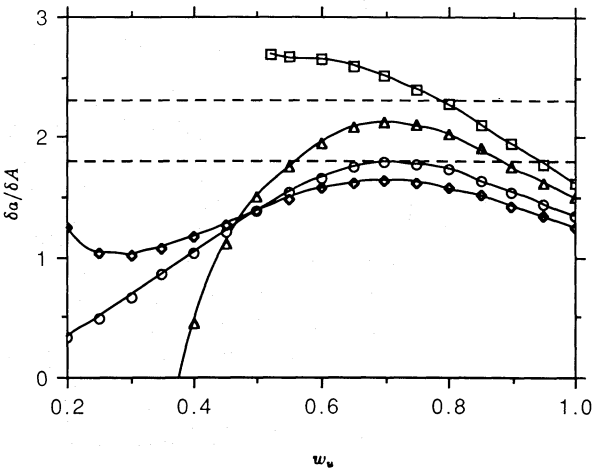

Fig. 8a. The ratio $\delta a/\delta A$ of the Stokes V profile of Fe I 5250.2 Å averaged between $r=0$ and $r=4$ vs. w_u, the weight of the internal upflow velocity component. $w_u=1$ signifies that only an upflow is present, while $w_u=0.5$ means that up- and downflows have equal weight. The atmosphere within the flux tube is represented by the network model with $B(\tau=1)=2000$ G, while $\Delta T_{\rm ext}=-300$ K. $v_{\rm int}=\pm 1$ km s^{-1} for all the plotted curves, while $v_{\rm ext}=0$ km s^{-1} (squares), 0.5 km s^{-1} (triangles), 1.0 km s^{-1} (circles) and 1.5 km s^{-1} (diamonds). Only those points have been plotted for which both δa and δA are positive. Note that for $v_{\rm ext}=0$, $\delta a/\delta A$ is undefined at $w_u=0.5$. The horizontal dashed lines represent the observations

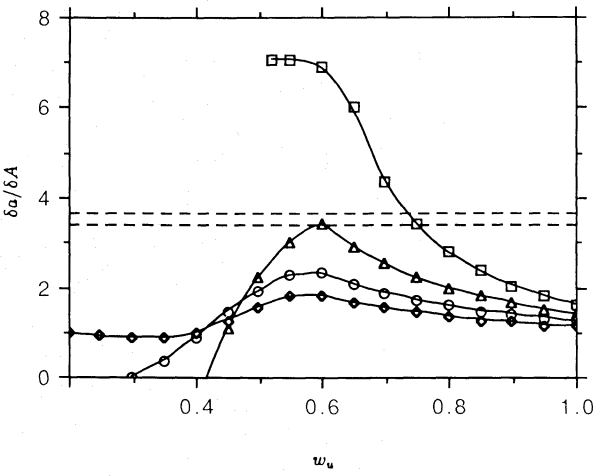

Fig. 8b. The same as Fig. 8a for Fe I 5083.3 Å

relatively small v_{ext} values ($\lesssim 0.5$ km s^{-1}). The $\delta a/\delta A$ observations of both lines can be approximately reproduced by the model with $v_{ext}=0.5$ km s^{-1} between $w_u \approx 0.55$ and $w_u \approx 0.65$ and by the model with $v_{ext}=0$ for $0.7 \lesssim w_u \lesssim 0.8$. The case of $v_{ext}=0$ is particularly interesting, since it is the case of a pure wave or oscillation. By studying this case the suggestion made by Solanki and Stenflo (1984) can be tested that waves or overstable oscillations inside magnetic elements are the dominant source of the Stokes V asymmetry. But first, let me briefly discuss the influence of the two time-component wave on the Stokes V zero-crossing wavelength and the line width.

Unfortunately, the zero-crossing wavelength is no longer conserved when the up- and downflow phases are not equally weighted. Zero-crossing wavelength shifts are minute when the weighting of the two phases is nearly the same and have exactly the value of v_{int} when only one of the two phases is present, irrespective of v_{ext}. This result can be proved for a height independent v_{int} with a similar argument as used by Grossmann-Doerth et al. (1988, 1989b) to prove that flows outside magnetic elements do not shift Stokes V.

The zero-crossing wavelength shifts of Fe I 5083.3 Å and 5250.2 Å in velocity units, $v_\lambda = c\,(\lambda_V - \lambda_0)/\lambda_0$, are plotted vs. w_u in Fig. 9 for $v_{ext}=0$. Not surprisingly the averaged V profiles are unshifted for $w_u=0.5$. Also, all four cases plotted in Fig. 8 ($v_{ext}=0.0$, 0.5, 1.0 and 1.5) give rather similar v_λ curves. Only one curve for each spectral line has been plotted, since it is unclear whether the minor differences between the curves of the four cases are real or only numerical artefacts. Due to the antisymmetry of these two curves around $w_u=0.5$ only half of the w_u range has been plotted. As can be seen from Fig. 9 the observational upper limit of ± 250 m s^{-1} on v_λ (marked by the horizontal dashed line) implies that only calculations with w_u values between approximately 0.4 and 0.6 need be considered further, as far as a comparison with the observational data is concerned. The fact that the observed $\delta a/\delta A$ values are better reproduced when the upflow is more strongly weighted means that the resulting Stokes V proriles are somewhat blueshifted. For Fe I 5250.2 Å the blueshift of the profile with the $\delta a/\delta A$ value closest to the observations is approximately 150–250 m s^{-1} ($v_{ext}=0.5$ km s^{-1}), and lies just below the upper limit set by the observations (e.g., Solanki, 1986). For Fe I 5083.3 Å, the blueshift of the corresponding profile is considerably smaller (50–100 m s^{-1}).

The width of the I_V profile as a function of w_u is plotted in Fig. 10 for Fe I 5250.2 Å and for three different v_{int} values: $v_{int}=\pm 0.5$ km s^{-1} (squares), ± 1.0 km s^{-1} (circles) and ± 1.5 km s^{-1} (triangles). $v_{ext}=0.5$ km s^{-1} for all three curves. $v_D\,(I_V)$ is largest close to $w_u=0.5$, i.e. when up- and downflow are given almost, but not necessarily quite equal weight. As expected, the Stokes V line widths increase with increasing "wave" amplitude. $w_u=1.0$ (pure internal upflow) forms an exception, with $v_D\,(I_V)$ decreasing as v_{int} is increased. A similar effect was noted for a purely external flow (Sect. 3.1). For $v_{int}=\pm 1.5$ km s^{-1} the largest I_V width agrees well with the observed value (this is also true for the Fe I 5083.3 Å width for the same model). Note that some difference is expected between this v_{int} value and the ξ_{mac} values obtained from fits to Stokes V or I_V, since a ξ_{mac} velocity distribution generally has a Gaussian or Voigt profile form with a large weight being given to small velocities. To achieve the broadening produced by a given v_{int} a larger ξ_{mac} value is required.

Let me now return to the case of $v_{ext}=0$. It follows from Fig. 8 that the calculated $\delta a/\delta A$ ratio is much too large for both lines in

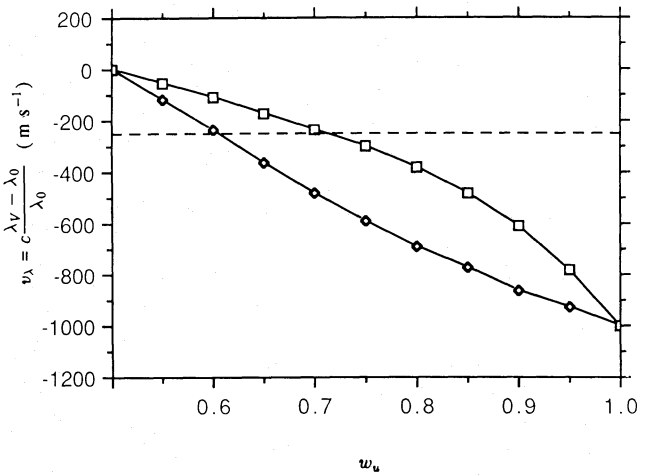

Fig. 9. The Stokes V zero-crossing shift, v_λ, in km s^{-1} vs. w_u. $v_\lambda = c(\lambda_V - \lambda_0)/\lambda_0$, where λ_V is the Stokes V zero-crossing wavelength, λ_0 is the unshifted standard wavelength of the line and c is the speed of light. Squares: Fe I 5083.3 Å, diamonds: Fe I 5250.2 Å. The atmospheric parameters are the same as in Fig. 8a, with $v_{ext}=0$. Other v_{ext} values give similar curves. Due to the antisymmetry of these curves only $w_u > 0.5$ has been shown. The observational upper limit on $|v_\lambda|$ is represented by the dashed line

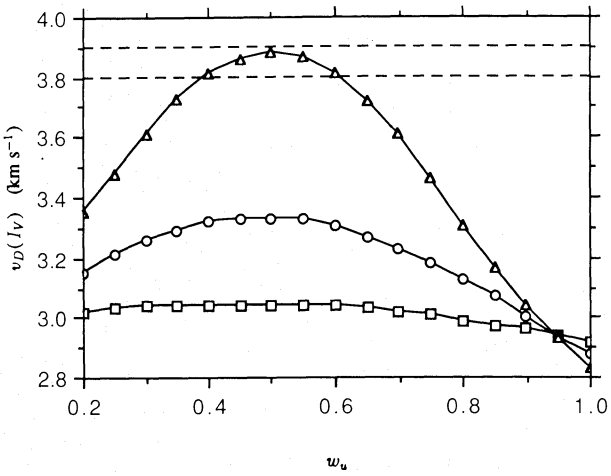

Fig. 10. Line width of the I_V profile, $v_D\,(I_V)$ of Fe I 5250.2 Å, in km s^{-1} vs. w_u. For the plotted curves $v_{ext}=0.5$ km s^{-1}, while v_{int} has the values 0.5 km s^{-1} (squares), 1.0 km s^{-1} (circles) and 1.5 km s^{-1} (triangles). Note that although for most w_u values $v_D\,(I_V)$ increases with increasing v_{int}, for $w_u=1$ (i.e. a pure upflow in the magnetic element) the opposite is the case. The observations are represented by the horizontal dashed line

the w_u range allowed by the zero-crossing wavelength ($0.4 \lesssim w_u \lesssim 0.6$). In addition, δA itself is much too small in this w_u range for $v_{int}=1$ km s^{-1}. Considerably larger v_{int} are required to match the observed values of δA, but these then increase the zero-crossing shifts and the line widths at a given w_u. These calculations therefore suggest that a model with a wave or oscillation in the tube alone would have great difficulty in reproducing the data, without the additional presence of an external downflow. Conversely, as shown in Sect. 3, an external downflow alone is not

sufficient either. Consequently, a combination of an internal wave-like motion and an external downflow is necessary.

In summary, it has been possible to greatly enhance the fit to both $\delta a/\delta A$ and to v_D (I_V) by combining appropriate v_{ext} and v_{int} values. An external downflow of approximately $0.5-1.0\,km\,s^{-1}$ and an internal wave of amplitude between $1\,km\,s^{-1}$ and $1.5\,km\,s^{-1}$ with a weight of the upflow phase, w_u, of 0.55–0.6 are required to reproduce of the plage data. The network data may require larger v_{ext} amplitudes. The smaller S/N in that dataset makes the determined values more uncertain. However, despite the success of the model, there are still some problems. For example, the parameters which reproduce the data for Fe I 5250.2 and 5083.3 Å, do not enhance $\delta a/\delta A$ of Fe II 5197.6 Å sufficiently. It only reaches a value of approximately 3 instead of the observed 4–6. The blueshift of Fe I 5250.2 Å is also somewhat uncomfortable. A simple possible solution of this last problem makes use of a finite flux tube boundary. In all the models considered here the boundary of the flux tube was made extremely thin and care was taken that v_{ext} and B do not overlap in this layer. In reality, this need not be so. A boundary layer of approximately 10 km thickness is expected to be present (see Schüssler, 1986), over which B and v_{ext} may overlap, leading to a slight redshift of Stokes V. Whether this effect is sufficiently strong to counteract the blueshift, remains to be seen, since it acts on the canopy profiles only. Of course, the remaining problems may simply be a result of the primitive "wave" model used in the present study.

4.3. Two-dimensional vs. one-dimensional models

The present calculations demonstrate the importance of 2-D models and line profile calculations along multiple rays for any attempt to quantitatively reproduce the observed Stokes V asymmetry observed outside sunspots. The importance of 2-D models for the broad-band circular polarization observed in sunspots is already well established (e.g., Landmann and Finn, 1979; Henson and Kemp, 1984; Makita, 1986; Skumanich and Lites, 1987). However, despite this and the pioneering efforts of Caccin and Severino (1979), Rees and Semel (1979) and Van Ballegooijen (1985a), most line profile calculations in magnetic elements have been carried out using 1-D models. 1-D flux tube models, like those of Solanki and Pahlke (1988) and Sánchez Almeida et al. (1988, 1989), miss one of the major sources of Stokes V asymmetry in magnetic elements, namely the large B and v gradients at the lower boundary of the canopy. This reflects unsuitably on the reliability of results obtained by 1-D models even if only velocities inside magnetic elements are assumed to be present in the model!

As an illustration I consider an upflow within a flux tube with the classical field geometry (expansion with height). Let, for simplicity, the upflow velocity be constant with height and let $v_{ext}=0$. In the typical 1-D model, which takes the axis of the flux tube to be representative of the whole structure, the Stokes V profiles will be shifted by an amount corresponding to this upflow, but they will remain exactly antisymmetric. In a proper 2-D model, the Stokes V profile averaged over multiple rays (or multiple lines-of-sight) show a substantial asymmetry, due to the combined B and v_{int} gradients at the canopy boundary. For example, if $v_{int}=-1\,km\,s^{-1}$, $v_{ext}=0$ and $\Delta T_{ext}=-300\,K$, then for Fe I 5250.2 Å and 5083.3 Å, δA values of around 8–9% are obtained. These values are of the order of the observed δA or even somewhat larger. The presence of a flux tube boundary obviously has a major effect on the asymmetry of the Stokes V profile and its neglection makes the results of 1-D calculations of, at the most, qualitative interest.

5. Discussion and conclusion

In the present paper the origin of the Stokes V asymmetry observed near disk centre in solar active regions and in the quiet network is studied with the help of a 2-D flux tube model of solar magnetic elements. The model incorporates the expansion of the magnetic field with height. It is shown that the observed relative area and amplitude asymmetry, the zero-crossing wavelengths and the widths of four Fe I and II Stokes V profiles belonging to lines with widely different properties can be reproduced relatively well within the framework of this model if it incorporates the following three features. Firstly, a downflow is present in the immediate surroundings of the magnetic elements. Secondly, this downflowing region is cooler than the quiet sun. Thirdly, an oscillatory or wave-like motion is present within the magnetic elements. Since the thermal and magnetic structures of the model are empirically derived, this implies that the same model effectively also reproduces a host of other line parameters (e.g. magnetic and thermal line ratios, Zeeman splitting of infrared lines etc.).

The sensitivity of the Stokes V asymmetry to the thermal and velocity structure in and around solar magnetic elements is also demonstrated. It has revealed itself to be the Stokes V line parameter most sensitive to the atmosphere in the vicinity of magnetic elements. When combined with other diagnostics, like the Stokes V line width and zero-crossing wavelength, it also becomes a powerful diagnostic of the mass-motions inside the magnetic elements. This diagnostic capability has been used to derive, for the first time, values of the temperature and velocity in the immediate surroundings of magnetic elements at the height of line formation. It is found that this region is approximately 250–350 K cooler than the average quiet sun and contains a downflow of $0.5-1.5\,km\,s^{-1}$ near the walls of the magnetic elements. Information on regions further away from the magnetic element cannot be derived from Stokes V. The present analysis also provides, to my mind, the strongest observational support so far for the presence of large amplitude waves or oscillations inside magnetic elements. A velocity amplitude of $1-1.5\,km\,s^{-1}$ is derived for the oscillatory or wave-like motion within the tube on the basis of a simple two time-component model. It is expected that the true wave amplitude is larger, since it must compensate for the larger weighting of small velocities in a sinusoidal wave, so that the true wave amplitude possibly lies between 1 and $3\,km\,s^{-1}$. The observations also suggest that the temperature in the upflowing and downflowing phases is probably not the same. Such a difference may be produced, for example, by radiative damping of the wave. These results must be considered preliminary, since most of the calculations carried out here are exploratory in nature and I have often been satisfied with reproducing the data only approximately.

Steep gradients in magnetic field strength, B, and velocity, v, extending over a short height in the atmosphere are found to be very efficient in producing δA, more efficient than gentler gradients extending over larger heights, which have generally been studied in the past. Consequently, the success of the 2-D model also provides further (indirect) support for current sheet bounded flux tube models of solar magnetic elements (e.g. Spruit,

1976; Deinzer et al., 1984b; Steiner et al., 1986; Knölker et al., 1988; Steiner and Pizzo, 1989), as opposed to models with a gradual horizontal decline in field strength and often no fixed boundary (e.g. Solanki, 1982; Osherovich et al., 1983; Steiner et al., 1986). This is in agreement with the empirical results of Zayer et al. (1989) and Solanki et al. (1989).

One consequence of the current analysis is that it shows the importance of 2-D models, at least as far as the Stokes V asymmetry is concerned. As pointed out earlier by Van Ballegooijen (1985a, b), the true influence of the atmosphere, and in particular the velocity, outside the magnetic elements on the Stokes V profile can only be judged in 2-D models. In addition, it is demonstrated in Sect. 4.3 that a 2-D model is essential for obtaining the quantitatively correct Stokes V asymmetry, even if only velocities within the magnetic elements are considered. Neglecting the expansion of the field and the steep gradients in B and v at its boundary to the external medium, as has generally been done in the past (e.g. Solanki and Pahlke, 1988; Sánchez Almeida et al., 1988, 1989) seriously affects the results, so that 1-D calculations of the Stokes V asymmetry are of qualitative value only. However, in many other respects Stokes V shows itself to be rather insensitive to conditions outside the magnetic elements. For example, Stokes V width reacts only mildly to external velocity amplitudes, distributions and gradients. Also, the Stokes V wing amplitudes and areas, as well as the I_V equivalent width, react relatively feebly to the external temperature, compared to their reaction to the internal temperature. This suggests that for some purposes, for which V asymmetry is unimportant and the Zeeman splitting is not too large (cf. Zayer et al., 1989; Grossmann-Doerth et al., 1989a), 1-D models may serve a useful role at solar disk centre. However, it is important to realise that if V profiles of lines formed at different heights are to be compared with each other in a 1-D model, then generally a B independent of height must be chosen, or incorrect results may be obtained (since V is proportional to the magnetic flux at the height of line formation, which, for small Zeeman splitting and a 1-D model, is in turn proportional to the field strength).

Let me now list some of the advantages and successes of the present model.

— An area asymmetry (δA) of the observed magnitude can be reproduced with reasonable values of the downflow velocity in the surroundings of the magnetic elements ($0.5-1.5\ \mathrm{km\,s^{-1}}$).

— Near disk centre, the detailed form of the velocity profile is not very important as long as the boundary of the magnetic element is relatively well defined and the velocity has, on average, the right value within a distance of a contribution function width from the flux tube boundary.

— In contrast to models with stationary flows within the flux tubes, mass conservation is no problem, and the proper area asymmetry can be reproduced without any zero-crossing shift if only downflows outside the model are considered (Grossmann-Doerth et al., 1988, 1989b). The zero-crossing shifts can still be kept to a reasonably small value, even if a sizeable part of the amplitude asymmetry is produced by motions within the magnetic elements.

— The present calculation of Stokes V asymmetry in magnetic elements is the first which takes the conservation of magnetic flux explicitely into account.

— The field strength and temperature stratifications within the model flux tube have not been chosen in an adhoc manner, but are based on comparisons with other Stokes V parameters (Solanki, 1986; Solanki et al., 1987, 1989; Zayer et al., 1989). The present model, therefore, fulfills a wide variety of observational constraints.

— The information on the structure of the magnetic elements and their surroundings derived from the present analysis agrees well with the knowledge obtained from magnetograms, filtergrams and white light images. Thus, the correlation between magnetograms, Dopplergrams and continuum pictures seen by Title et al. (1987) led them to conclude that magnetic elements are preferrably located in dark and downflowing intergranular lanes. Earlier, various authors had noted the correlation between filigree and dark intergranular lanes (e.g. Mehltretter, 1974; Dunn and Zirker, 1974) and between continuum bright points and dark lanes (Muller, 1983; Von der Lühe, 1989). In contrast to the above observations the Stokes V asymmetry is a quantitative diagnostic, i.e. it can be used to derive the temperature and downflow velocity in the intergranular lanes close to the magnetic elements.

The present results also strengthen the observational case for the presence of oscillations or waves within magnetic elements. Earlier observational evidence has been somewhat equivocal. Direct observations have been restricted to either 5 minute oscillations, or small amplitude waves excited by these oscillations (Giovanelli et al., 1978; Wiehr, 1985; cf. Roberts, 1983), so that line broadening has previously constituted the only (indirect) evidence for large amplitude non-stationary mass motions (Solanki, 1986). The large Stokes V $\delta a/\delta A$ ratio provides additional evidence for the presence of non-stationary mass motions, since it explicitly requires up- and downflow phases, and cannot be explained simply by turbulent broadening.

— The picture of solar magnetic elements emerging from the present use of the Stokes V asymmetry as a diagnostic is highly appealing, since it fits in very well with out present theoretical understanding of such structure (cf. e.g. Spruit, 1983; Spruit and Roberts, 1983; Schüssler, 1986, 1987; Solanki, 1987b, for reviews). Theoretically, a magnetic element expands with height and the granular flow field is expected to concentrate field lines into the intergranular lanes (cf. Nordlund, 1983, 1986). This is also the most suitable place for the initial downflow leading to a convective collapse and the resulting kG field strengths (e.g. Parker, 1978; Webb and Roberts, 1978; Spruit, 1979; Hasan, 1985). A cooling of the flux tube surroundings is expected directly due to the influx of radiation into the tube (Deinzer et al., 1984b; Grossmann-Doerth et al., 1989a; Steiner, 1989). This cooling also drives a baroclinic flow, which is mainly a downflow in the vicinity of the magnetic elements (Deinzer et al., 1984b). Finally, oscillations and waves within magnetic elements have often been proposed on theoretical grounds. Flux tube waves are among the main contenders to heat the chromosphere and the corona (e.g., Cram and Damé, 1983; Herbold et al., 1985; Zähringer and Ulmschneider, 1987; Rammacher and Ulmschneider, 1989; cf. Spruit and Roberts, 1983, for a review). Waves have been calculated in flux tubes by a number of authors (for reviews see e.g. Roberts, 1984, 1986; Thomas, 1985; Ulmschneider and Muchmore, 1986). Overstable oscillations have also been considered in detail theoretically. They are expected to be produced automatically as the final stage of the convective collapse (Spruit, 1979; Hasan, 1984, 1985).

The present model calculations also have some weaknesses. For example, a considerably larger number of lines must be considered if more accurate values of T_{ext}, v_{ext}, etc. are to be

derived. Very probably $T_{ext}(\tau)$ is not parallel to $T_{HSRA}(\tau)$ as has been assumed here. Even $T_{int}(\tau)$ is not entirely certain (cf. e.g., Solanki, 1987a; Keller, 1988) and other models will also have to be considered in future. Furthermore, in the present models a temperature-jump is present at the flux tube boundary which is artificial and may affect the results. However, the main shortcoming is the rather simple treatment of the non-stationary mass-motions inside the magnetic element. A two component, height independent velocity probably constitutes only a rudimentary description of nature, and a more physically consistent model is required. Calculations with longitudinal tube waves (cf. Roberts and Webb, 1979; Webb and Roberts, 1980; Roberts, 1983), whose amplitudes depend on height form an important next step. Indeed, our knowledge of the influence of waves in general on the Stokes profiles (other than Stokes *I*) is practically non-existent. Such an investigation is currently underway and will be the subject of a future publication. The present model and the low spatial resolution FTS data also cannot decide between truly non-stationary motions or a distribution of stationary up- and downflows (e.g. siphon flows, as studied by Thomas, 1988). In view of these shortcomings and the fact that the calculations carried out here must in many ways be considered exploratory, it is hardly surprising that not all the line parameters of all the lines are equally well reproduced. For example, the calculated $\delta a/\delta A$ value of Fe II 5197.6 Å still falls somewhat short of the observed value.

It must also be noted that the properties derived from the asymmetry of relatively low spatial resolution Stokes *V* profiles refer only to some average over an ensemble of magnetic elements. The velocities in and around individual elements may depart considerably from this mean. Also, the relative insensitivity of the asymmetry to the details of the external velocity constitutes a disadvantage as far as the diagnosis of the same detailed external velocity structure is concerned.

There are still a number of questions left unanswered by the present analysis. Some of them concern our basic understanding of how the Stokes *V* asymmetry is produced in a complex 2-D situation. One question which has not been addressed at all in the present paper is the striking centre to limb variation (CLV) of the Stokes *V* asymmetry. δA and δa both change sign near the limb (Stenflo et al., 1987a; Pantellini et al., 1988). At least three different mechanisms come to mind whereby the sign of the asymmetry can be reversed near the limb without contradicting the disk centre results of the present model. The CLV may be a result of seeing higher in the atmosphere near the limb. This can change the sign of δA if the external flow velocity changes sign at greater heights (i.e. it becomes an upflow closer to the temperature minimum level). Another feature which may produce the observed effect is a horizontal component of the velocity (e.g. an inflow towards the magnetic element). Finally, the CLV of δA may to a large extent simply be due to the different angle between the field and the line of sight near the limb (cf. Auer and Heasley, 1978; Skumanich and Lites, 1987).

Acknowledgements. It is a pleasure to acknowledge fruitful discussions with Uli Grossmann-Doerth and Manfred Schüssler. I am also indepted to Jan Stenflo and the Three Musketeers (Manolo Collados, José Carlos Del Toro Iniesta, Jorge Sánchez Almeida) for carefully reading the manuscript.

References

Auer, L.H., Heasley, J.H.: 1978, *Astron. Astrophys.* **64**, 67
Beckers, J.M.: 1969a, *Solar Phys.* **9**, 372
Beckers, J.M.: 1969b, *Solar Phys.* **10**, 262
Blackwell, D.E., Ibbetson, P.A., Petford, A.D., Shallis, M.J.: 1979 *Monthly Notices Roy. Astron. Soc.* **186**, 633
Blackwell, D.E., Petford, A.D., Shallis, M.J.: 1979, *Monthly Notices Roy. Astron. Soc.* **186**, 657
Brandt, P.N., Solanki, S.K.: 1989, *Astron. Astrophys.* (submitted)
Caccin, B., Severino, G.: 1979, *Astrophys. J.* **232**, 297
Chapman, G.A.: 1979, *Astrophys. J.* **232**, 923
Cram, L.E., Damé, L.: 1983, *Astrophys. J.* **272**, 355
Defouw, R.J.: 1976, *Astrophys. J.* **209**, 266
Deinzer, W., Hensler, G., Schüssler, M., Weisshaar, E.: 1984a, *Astron. Astrophys.* **139**, 426
Deinzer, W., Hensler, G., Schüssler, M., Weisshaar, E.: 1984b, *Astron. Astrophys.* **139**, 435
Dunn, R.B., Zirker, J.B.: 1973, *Solar Phys.* **33**, 281
Gingerich, O., Noyes, R.W., Kalkofen, W., Cuny, Y.: 1971, *Solar Phys.* **18**, 347
Giovanelli, R.G.: 1980, *Solar Phys.* **68**, 49
Giovanelli, R.G., Livingston, W.C., Harvey, J.W.: 1978, *Solar Phys.* **59**, 49
Grossmann-Doerth, U., Knölker, M., Schüssler, M., Weisshaar, E.: 1989a, in *Solar and Stellar Granulation*, Proc. NATO Advanced Research Workshop, eds. R. Rutten, G. Severino, Reidel, Dordrecht (in press)
Grossmann-Doerth, U., Schüssler, M., Solanki, S.K.: 1988, *Astron. Astrophys. Letters* **206**, L37
Grossmann-Doerth, U., Schüssler, M., Solanki, S.K.: 1989b, *Astron. Astrophys.* (in press)
Hasan, S.S.: 1984, *Astrophys. J.* **285**, 851
Hasan, S.S.: 1985, *Astron. Astrophys.* **143**, 39
Hasan, S.S., Schüssler, M.: 1985, *Astron. Astrophys.* **151**, 69
Henson, G.D., Kemp, J.C.: 1984, *Solar Phys.* **93**, 289
Herbold, G., Ulmschneider, P., Spruit, H.C., Rosner, R.: 1985, *Astron. Astrophys.* **145**, 157
Holweger, H.: 1979, in *Proc. 22nd Liège International Astrophys. Symp.*, Inst. d'Astrophysique, Liège, p. 117
Holweger, H., Müller, E.A.: 1974, *Solar Phys.* **39**, 19
Illing, R.M.E., Landman, D.A., Mickey, D.L.: 1975, *Astron. Astrophys.* **41**, 183
Immerschitt, S., Schröter, E.H.: 1989, *Astron. Astrophys.* **208**, 307
Jones, H.P.: 1985, in *Chromospheric Diagnostics and Modelling*, ed. B.W. Lites, National Solar Obs., Sacramento Peak, NM, p. 175
Keil, S.L.: 1980, *Astrophys. J.* **237**, 1035
Keller, C.U.: 1988, Diplomarbeit, E.T.H. Zürich
Kemp, J.C., Macek, J.H., Nehring, F.W.: 1984, *Astrophys. J.* **278**, 863
Knölker, M., Schüssler, M., Weisshaar, E.: 1988, *Astron. Astrophys.* **194**, 257
Landi Degl'Innocenti, E.: 1985, in *Theoretical Problems in High Resolution Solar Physics*, ed. H.U. Schmidt, Max-Planck-Inst. f. Astrophys., Munich, p.162
Landman, D.A., Finn, G.D.: 1979, *Solar Phys.* **63**, 221
Lites, B.W., Skumanich, A., Rees, D.E., Murphy, G.A.: 1988, *Astrophys. J.* **330**, 493
Makita, M.: 1986, *Solar Phys.* **106**, 269
Mehltretter, J.P.: 1974, *Solar Phys.* **38**, 43

Montesinos, B., Thomas, J.H.: 1989, *Astrophys. J.* **337**, 977
Muller, R.: 1983, *Solar Phys.* **85**, 113
Nordlund, Å.: 1983, in *Solar and Stellar Magnetic Fields: Origins and Coronal Effects*, ed. J.O. Stenflo, *IAU Symp.* **102**, 79
Nordlund, Å.: 1986, in *Proc. Workshop on Small Magnetic Flux Concentrations in the Solar Photosphere*, eds. W. Deinzer, M. Knölker, H.H. Voigt, Vandenhoeck & Ruprecht, Göttingen, p. 83
Osherovich, V.A., Flå, T., Chapman, G.A.: 1983, *Astrophys. J.* **286**, 412
Pahlke, K.D., Solanki, S.K.: 1986, *Mitt. Astron. Ges.* **65**, 162
Pantellini, F.G.E., Solanki, S.K., Stenflo, J.O.: 1988, *Astron. Astrophys.* **189**, 263
Parker, E.N.: 1978, *Astrophys. J.* **221**, 368
Parker, E.N.: 1979, *Cosmical Magnetic Fields*, Clarendon Press, Oxford
Phillips, M.M.: 1979, *Astrophys. J. Suppl. Ser.* **39**, 377
Pierce, A.K., Breckinridge, J.B.: 1973, *KPNO Contr.* **559**
Pneuman, G.W., Solanki, S.K., Stenflo, J.O.: 1986, *Astron. Astrophys.* **154**, 231.
Rammacher, W., Ulmschneider, P.: 1989, in *Solar and Stellar Granulation*, Proc. NATO Advanced Research workshop, eds. R. Rutten, G. Severino, Reidel, Dordrecht (in press)
Rees, D.E., Semel, M.D.: 1979, *Astron. Astrophys.* **74**, 1
Roberts, B.: 1983, *Solar Phys.* **87**, 77
Roberts, B.: 1984, in *The Hydromagnetics of the Sun*, eds. T.D. Guyenne, J.J. Hunt, *Proc. Fourth European Meeting on Solar Physics*, ESA SP-220, 137
Roberts, B.: 1986, in *Small Scale Magnetic Flux Concentrations in the Solar Photoshpere*, eds. W. Deinzer, M. Knölker, H.H. Voigt, Vandenhoeck & Ruprecht, Göttingen, p. 169
Roberts, B., Webb, A.R.: 1979, *Solar Phys.* **64**, 77
Sánchez Almeida, J., Collados, M., Del Toro Iniesta, J.C.: 1988, *Astron. Astrophys.* **201**, L37
Sánchez Almeida, J., Collados, M., Del Toro Iniesta, J.C.: 1989, *Astron. Astrophys.* (in press)
Schüssler, M.: 1986, in *Small Scale Magnetic Flux Concentrations in the Solar Photosphere*, eds. W. Deinzer, M. Knölker, H.H. Voigt, Vandenhoeck & Ruprecht, Göttingen, p. 103
Schüssler, M.: 1987, in *The Role of Fine-Scale Magnetic Fields on the Structure of the Solar Atmosphere*, eds. E.-H. Schröter, M. Vázquez, A.A. Wyller, Cambridge University Press, Cambridge, p. 223
Schüssler, M., Solanki, S.K.: 1988, *Astron. Astrophys.* **192**, 338
Simmons, G.J., Blackwell, D.E.: 1982, *Astron. Astrophys.* **112**, 209
Skumanich, A., Lites, B.W.: 1987, *Astrophys. J.* **322**, 483
Solanki, S.K.: 1982, Diplomarbeit, ETH, Zürich
Solanki, S.K.: 1985, in *Theoretical Problems in High Resolution Solar Physics*, ed. H.U. Schmidt, Max-Planck-Inst. f. Astrophys., Munich, p. 172
Solanki, S.K.: 1986, *Astron. Astrophys.* **168**, 311
Solanki, S.K.: 1987a, in *The Role of Fine-Scale Magnetic Fields on the Structure of the Solar Atmosphere*, eds. E.-H. Schröter, M. Vázquez, A.A. Wyller, Cambridge University Press, Cambridge, p. 67
Solanki, S.K.: 1987b, in *Proc. Tenth European Regional Astronomy Meeting of the IAU. Vol. 1: The Sun*, eds. L. Hejna, M. Sobotka, Publ. Astron. Inst. Czechoslovak Acad. Sci., p. 95
Solanki, S.K.: 1987c, Ph.D. Thesis, ETH, Zürich
Solanki, S.K., Keller, C., Stenflo, J.O.: 1987, *Astron. Astrophys.* **188**, 183
Solanki, S.K., Pahlke, K.D.: 1988, *Astron. Astrophys.* **201**, 143
Solanki, S.K., Steenbock, W.: 1988, *Astron. Astrophys.* **189**, 243
Solanki, S.K., Stenflo, J.O.: 1984, *Astron. Astrophys.* **140**, 185
Solanki, S.K., Stenflo, J.O.: 1985, *Astron. Astrophys.* **148**, 123
Solanki, S.K., Stenflo, J.O.: 1986, *Astron. Astrophys.* **170**, 120
Solanki, S.K., Zayer, I., Stenflo, J.O.: 1989, in *Proc. 10th Sacramento Peak Workshop*, ed. O. von der Lühe (in press)
Spruit, H.C.: 1974, *Solar Phys.* **34**, 277
Spruit, H.C.: 1976, *Solar Phys.* **50**, 269
Spruit, H.C.: 1979, *Solar Phys.* **61**, 363
Spruit, H.C.: 1983, in *Solar and Steller Magnetic Fields: Origins and Coronal Effects*, ed. J.O. Stenflo, *IAU Symp.* **102**, 41
Spruit, H.C., Roberts, B.: 1983, *Nature* **304**, 401
Steiner, O.: 1989, *Astron. Astrophys.* (submitted)
Steiner, O., Pneuman, G.W., Stenflo, J.O.: 1986, *Astron. Astrophys.* **170**, 126
Steiner, O., Pizzo, V.J.: 1989, *Astron. Astrophys.* (in press)
Stenflo, J.O., Harvey, J.W.: 1985, *Solar Phys.* **95**, 99
Stenflo, J.O., Harvey, J.W., Brault, J.W., Solanki, S.K.: 1984, *Astron. Astrophys.* **131**, 333
Stenflo, J.O., Lindegren, L.: 1977, *Astron. Astrophys.* **59**, 367
Stenflo, J.O., Solanki, S.K., Harvey, J.W.: 1987a, *Astron. Astrophys.* **171**, 305
Stenflo, J.O., Solanki, S.K., Harvey, J.W.: 1987b, *Astron. Astrophys.* **173**, 167
Thomas, J.H.: 1985, in *Theoretical Problems in High Resolution Solar Physics*, ed. H.U. Schmidt, Max-Planck-Inst. f. Astrophys., Munich, p. 126
Thomas, J.H.: 1988, *Astrophys. J.* **333**, 407
Title, A.M., Tarbell, T.D., Topka, K.P.: 1987, *Astrophys. J.* **317**, 892
Ulmschneider, P, Muchmore, D.: 1986, in *Small Scale Magnetic Flux Concentrations in the Solar Photosphere*, eds. W. Deinzer, M. Knölker, H.H. Voigt, Vandenhoeck & Ruprecht, Göttingen, p. 191
Unsöld, A.: 1955, *Physik der Sternatmosphären*, Springer, Berlin, Heidelberg
Van Ballegooijen, A.A.: 1985a, in *Measurements of Solar Vector Magnetic Fields*, ed. M.J. Hagyard, NASA Conf. Publ. 2374, p. 322
Van Ballegooijen, A.A.: 1985b, in *Theoretical Problems in High Resolution Solar Physics*, ed. H.U. Schmidt, Max-Planck-Inst. f. Astrophys., Munich, p. 177
Von der Lühe, O.: 1989, in *Proc. 10th Sacramento Peak Workshop*, ed. O. von der Lühe (in press)
Webb, A.R., Roberts, B.: 1978, *Solar Phys.* **59**, 249
Webb, A.R., Roberts, B.: 1980, *Solar Phys.* **68**, 87
Wiehr, E.: 1985, *Astron. Astrophys.* **149**, 217
Zähringer, K., Ulmschneider, P.: 1987, in *The Role of Fine-Scale Magnetic Fields on the Structure of the Solar Atmosphere*, eds. E.-H. Schröter, M. Vázquez, A.A. Wyller, Cambridge University Press, Cambridge, p. 243
Zayer, I., Solanki, S.K., Stenflo, J.O.: 1989, *Astron. Astrophys.* **211**, 463